

ASDF: A Compiler for Qwerty, a Basis-Oriented Quantum Programming Language

Austin J. Adams*

Georgia Institute of Technology
Atlanta, GA, USA
aja@gatech.edu

Sharjeel Khan

Georgia Institute of Technology
Atlanta, GA, USA
smkhan@gatech.edu

Arjun S. Bhamra

Georgia Institute of Technology
Atlanta, GA, USA
abhamra@gatech.edu

Ryan R. Abusaada

Georgia Institute of Technology
Atlanta, GA, USA
rabusaada6@gatech.edu

Anthony M. Cabrera

Oak Ridge National Laboratory
Oak Ridge, TN, USA
cabreraam@ornl.gov

Cameron C. Hoechst

Georgia Institute of Technology
Atlanta, GA, USA
choechst3@gatech.edu

Travis S. Humble

Oak Ridge National Laboratory
Oak Ridge, TN, USA
humblets@ornl.gov

Jeffrey S. Young

Georgia Institute of Technology
Atlanta, GA, USA
jyoung9@gatech.edu

Thomas M. Conte

Georgia Institute of Technology
Atlanta, GA, USA
conte@gatech.edu

Abstract

Qwerty is a high-level quantum programming language built on bases and functions rather than circuits. This new paradigm introduces new challenges in compilation, namely synthesizing circuits from basis translations and automatically specializing adjoint or predicated forms of functions. This paper presents ASDF, an open-source compiler for Qwerty that answers these challenges in compiling basis-oriented languages. Enabled with a novel high-level quantum IR implemented in the MLIR framework, our compiler produces OpenQASM 3 or QIR for either simulation or execution on hardware. Our compiler is evaluated by comparing the fault-tolerant resource requirements of generated circuits with other compilers, finding that ASDF produces circuits with comparable cost to prior circuit-oriented compilers.

1 Introduction

Qwerty is a recently proposed, Python-embedded, high-level quantum programming language built on quantum basis translations rather than quantum gate circuitry [2]. Although the language provides a valuable scaffold for reasoning about quantum algorithms, its compilation is challenging due to several fundamental constructs. Chief among these constructs is its *basis translation*, a novel transformation that shifts qubits from one basis to another, which the compiler must synthesize as a quantum circuit. In addition, functions in Qwerty may be invoked backward or in a predicated form, requiring the compiler to generate *function specializations*. However, modern quantum compilers cannot compile basis translations and their synthesis of function specializations is more constrained. Moreover, current intermediate representations (IRs) for quantum programs are ill-suited to represent

Qwerty programs due to the semantic gap between Qwerty and quantum circuits.

This paper presents *ASDF*¹, the first compiler for Qwerty’s new basis-oriented quantum programming paradigm. ASDF spans the chasm between high-level code expressed with functions and bases and efficient low-level circuits by leveraging a novel quantum IR design implemented in the MLIR framework. We evaluate the efficiency of circuitry produced by ASDF in industry-standard formats such as OpenQASM 3 and QIR across a suite of well-known quantum algorithms written in Qwerty, finding ASDF’s output competitive with handwritten assembly.

The backbone of ASDF is a runtime that retrieves the Python AST (abstract syntax tree) [13] and type checks it to enforce quantum semantics and prevent violation of the postulates of quantum computation. Type checking Qwerty’s quantum constructs could result in exponential runtime, but we present an efficient type checker that uses quantum basis factorization to avoid this pitfall. Because of the nature of quantum algorithm expression in Qwerty, the Qwerty AST consists of a pipeline of function calls, which ASDF must rebuild into a more imperative structure for downstream compatibility. We tackle this challenge by integrating a custom IR dialect into MLIR such that function reversal and predication are computed in full generality. Aggressive inlining aiming to linearize the computation lowers this IR into a quantum dataflow description of the quantum circuit, where peephole optimizations are applied to gate subgraphs to reduce the complexity and improve the quality of the output. An imperative circuit description can be easily generated from this dataflow graph; two formats are implemented. One is standard OpenQASM3 that can be sent directly to IBM for execution [9, 19]. The other is QIR, which can be input to

*Corresponding author

¹ “ASDF” is a keyboard pun on “Qwerty.”

QIR-EE to target several different hardware and simulation platforms [21, 61]. The source code for ASDF is available at <https://github.com/gt-tinker/qwerty>.

This paper makes the following contributions:

- Type checking basis translations efficiently to avoid exponential runtime;
- *Qwerty IR*, an IR designed both to represent the unique structure of Qwerty programs and to flatten easily into a quantum circuit;
- Reversing or predicating quantum basic blocks effectively;
- Novel techniques for synthesizing circuits for basis translations with minimal overhead; and
- A demonstration that the compiled code is of equal quality to handwritten quantum circuits in Qiskit, Quipper, and Q# for several well-known quantum algorithms [16, 38, 53].

The following section presents a brief introduction to quantum notation followed by an overview of Qwerty. Afterward, an overview of the ASDF compiler is provided and each compilation phase is discussed. Empirical comparisons of the compiler’s output to hand-built circuits are then presented, followed by a discussion of related work and overall conclusions.

2 Background and Motivation

2.1 Quantum Computing Notation

For a thorough introduction to quantum computing and its notation, we direct readers to Chapters 1 and 2, respectively, of Nielsen and Chuang [34]. However, some definitions are included here for clarity. We define the *Z eigenbasis* as $|0\rangle/|1\rangle$; the *X eigenbasis* as $|+\rangle/|-\rangle$ (or equivalently $|p\rangle/|m\rangle$); and the *Y eigenbasis* as $|i\rangle/|j\rangle$, where $|i\rangle = \frac{1}{\sqrt{2}}(|0\rangle + i|1\rangle)$ and $|j\rangle = \frac{1}{\sqrt{2}}(|0\rangle - i|1\rangle)$ [34]. We call the first vector in each of these pairs the *plus eigenstate* (since it has eigenvalue +1 for the respective Pauli) and the second vector the *minus eigenstate* (since it has eigenvalue -1 for the respective Pauli). The relative phase shift gate $P(\theta)$ is defined as $|0\rangle\langle 0| + e^{i\theta} |1\rangle\langle 1|$ [49].

2.2 An Introduction to Qwerty

Although Qwerty is defined in prior work [2], a reference for relevant Qwerty features is included here for convenience, since it affects type checking (e.g., Section 4.1) and influences the design of our basis-oriented IR (Section 5).

As discussed above, Qwerty is a *basis-oriented* quantum programming language [2]. In contrast with prior quantum programming languages, Qwerty programmers write quantum programs using primitives defined in terms of orthonormal bases or classical logic, not by choosing from a library of quantum gates. (Fig. 1 is an example of a Qwerty program [2].)

```

1 import sys
2 from qwerty import *
3
4 def bv(secret_str):
5     @classical[N](secret_str)
6     def f(secret_str: bit[N], x: bit[N]) -> bit:
7         return (secret_str & x).xor_reduce()
8
9     @qpu[N](f)
10    def kernel(f: cfunc[N,1]) -> bit[N]:
11        return 'p'[N] | f.sign \
12            | pm[N] >> std[N] \
13            | std[N].measure
14
15    return kernel()
16
17 secret_str = bit.from_str(sys.argv[1])
18 print(bv(secret_str))

```

Figure 1. Bernstein–Vazirani expressed in Qwerty [2]

Every basis in Qwerty is grounded in four *primitive bases*: **std** (the *Z* eigenbasis), **pm** (the *X* eigenbasis), **ij** (the *Y* eigenbasis), and **fourier**[*N*] (the *N*-qubit Fourier basis [34, §5.1]). Each primitive basis can be used in a Qwerty *basis expression*: the tensor product of two bases is written $b_1 + b_2$, and the *N*-fold tensor product is written $b[N]$. Basis expressions may also contain *basis literals*, written $\{bv_1, bv_2, \dots, bv_m\}$ where $m > 0$. Each *basis vector* bv is a *qubit literal* with an optional complex unit scalar phase factor (written $bv@theta$ to evoke $bv \cup theta$). Qubit literals resemble string literals (e.g., '1010') and are sequences of **p**, **m**, **i**, **j**, **0**, and **1**, each *position* of this sequence corresponding to the vectors in Section 2.1. The *dimension* of a qubit literal, basis vector, or basis is its number of qubits. The *eigenbits* of a basis vector is a bitstring whose length is the dimension of the vector; each bit is set if and only if the corresponding position is a minus eigenstate. In a well-typed basis literal, all eigenbits must be distinct, all vector dimensions must be equal, and all positions of all vectors must have the same primitive basis (defined as the non-**fourier** primitive basis the respective position belongs to). A *canon form* of a basis is a sequence (tensor product) of *basis elements*, each of which is either a basis literal or a *built-in basis*, an *N*-qubit primitive basis (e.g., **pm**[4]). Any Qwerty basis can be written in canon form.

The core computational primitive of Qwerty is the *basis translation* [2]. Given an input basis b_{in} and an output basis b_{out} , a basis translation $b_{in} >> b_{out}$ performs the following operation (where the vectors $|b^{(i)}\rangle$ are the basis vectors of a basis b):

$$\begin{aligned}
 & \alpha_1 |b_{in}^{(1)}\rangle + \alpha_2 |b_{in}^{(2)}\rangle + \dots + \alpha_n |b_{in}^{(n)}\rangle + |b_{in}^\perp\rangle \\
 & \Downarrow \\
 & \alpha_1 |b_{out}^{(1)}\rangle + \alpha_2 |b_{out}^{(2)}\rangle + \dots + \alpha_n |b_{out}^{(n)}\rangle + |b_{in}^\perp\rangle
 \end{aligned}$$

That is, a basis translation preserves state amplitudes but translates the basis vectors from b_{in} to b_{out} ; amplitudes are preserved because all possible translations are unitary. This unitarity promise is accomplished by all Qwerty bases being orthonormal and Qwerty requiring that both bases in a basis translation span the same space: $\text{span}(b_{\text{in}}) = \text{span}(b_{\text{out}})$.

For example, the basis translation $\{ '01', '10' \} \gg \{ '10', '01' \}$ swaps two qubits, since it performs the following operation:

$$\begin{aligned} & \beta_1 |00\rangle + \alpha_1 |01\rangle + \alpha_2 |10\rangle + \beta_2 |11\rangle \\ & \Downarrow \\ & \beta_1 |00\rangle + \alpha_1 |10\rangle + \alpha_2 |01\rangle + \beta_2 |11\rangle \end{aligned}$$

This example is identical to a SWAP gate in circuit-level quantum programming.

In quantum algorithms, it is common to run a sequence of quantum operations backwards or in a proper subspace. Qwerty makes the intuitive choice to let these reversible (or predicatable) sequences of quantum operations be functions that take **qubits** and return **qubits**. All quantum operations in these reversible functions must themselves be reversible; such functions are designated by having the type $T_1 \xrightarrow{\text{rev}} T_2$ [2, §A]. A version of a reversible function f than runs backwards (i.e., an adjointed form) is written in Qwerty as $\sim f$. A version which runs only when the span of a basis b contains the state of some additional ($\dim b$) input qubits (i.e., a predicated form) is written as $b \ \& \ f$. Both take an operand of type **qubit**[N] $\xrightarrow{\text{rev}}$ **qubit**[N].

2.3 Motivation: Challenges in Compiling Qwerty

Programming in Qwerty requires a compiler that meets the following challenges:

1. **Handling bases:** The basis-oriented primitives in Qwerty must be *efficiently* type checked and lowered to gates, the standard quantum program representation expected by quantum compiler backends.
2. **Linearizing code:** The functional constructs in Qwerty code such as indirect calls, adjoint calls, and predicated calls must be converted into straight-line code as much as possible because functional features may not be well-supported in quantum hardware.
3. **Integration with standard tools:** For Qwerty to be practical, a compiler should produce quantum circuits in a format recognized by industry-standard tools such as QIR or OpenQASM.

The remainder of this paper is dedicated to how the design of ASDF addresses these challenges.

3 Overview of the ASDF Compiler

Fig. 2 illustrates the compilation process for a Qwerty program in the ASDF compiler. The figure is divided into regions of steps that correspond to the following sections of this paper: **Section 4** covers the generation and transformations

done on the abstract syntax tree (AST), notably including type checking. **Section 5** defines the high-level IR used to represent and optimize Qwerty programs (*Qwerty IR*), implemented as a dialect in MLIR. **Section 6** describes how Qwerty IR is lowered to a lower-level gate-based IR. This includes synthesizing circuits from basis translations and generating specializations (reversed and predicated forms) of functions. Finally, **Section 7** discusses how ASDF generates QIR and OpenQASM 3.

Frameworks used in implementation: The implementation of ASDF involves two frameworks commonly used for quantum compiler implementation, MLIR and QIR.

MLIR: The Multi-Level IR compiler framework, commonly called MLIR, is a popular and extensible compiler infrastructure within the LLVM project, and its design lends itself to supporting domain specific languages and IRs [26]. MLIR supports user-defined *dialects* containing reusable types, *attributes* (metadata known at compile time), and *ops* (instructions). Common optimizations ship with MLIR, including function inlining and *canonicalization*; the latter simplifies IR to better enable optimizations (e.g., through constant folding and dead code elimination). MLIR dialects exist for representing quantum programs using gates or domain-specific ops [19, 22, 23, 29, 36, 55].

QIR: ASDF is designed to produce Quantum Intermediate Representation (QIR), an LLVM IR-based quantum IR designed to be a target for high-level quantum programming languages such as Microsoft’s Q# [3, 28, 53]. To respect the capabilities of different hardware, QIR has different *profiles*, including the *Base Profile* [59], which allows only forward unconditional branching and bans dynamic qubit allocation, and the *Unrestricted Profile* [8], which permits the complete library of QIR intrinsics and full generality of LLVM IR.

4 Abstract Syntax Tree

AST generation: Compilation in ASDF begins similarly to to Python DSLs for classical accelerators such as Intrepyyd [65] or Triton [56]: ASDF retrieves the Python AST (itself a Python data structure) for **@qpu** kernels and **@classical** functions using the Python standard library [13]. (Thus, the ASDF compiler and runtime are distributed as a Python package, so no changes to the Python interpreter itself are needed.) While easy to manipulate, the Python AST is untyped and intended for Python programs, not Qwerty programs, so ASDF converts it to a typed Qwerty AST by recognizing the patterns in the AST formed by Qwerty syntax.

AST expansion: ASDF then preprocesses the AST in advance of type checking. Qwerty supports *dimension variables*, which allow defining a function polymorphically with respect to some integer dimension (e.g., input problem size). A Qwerty compiler should infer dimension variables based on the types of captures when possible — for example, ASDF

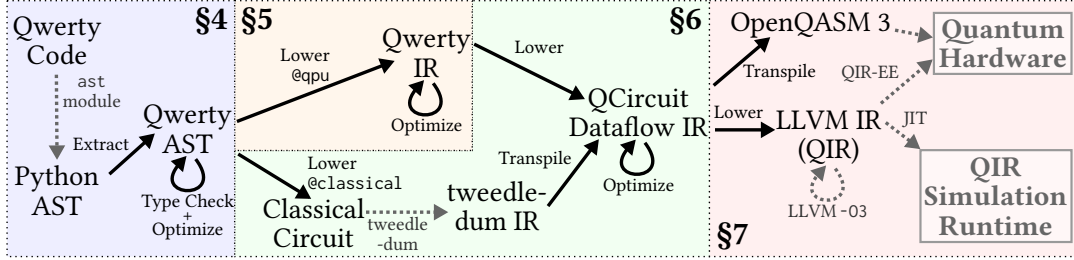


Figure 2. Compilation flow for our Qwerty compiler. Solid arrows are our work.

infers N from the length of the captured secret bitstring on lines 5-6 in Fig. 1. Once dimension variables are determined, whether by inference or by the programmer explicitly providing them, ASDF performs *expansion* on the AST, replacing all expressions involving dimension variables with constants. This includes unrolling loops and expanding $\text{expr}[N]$ to $\text{expr} + \text{expr} + \dots + \text{expr}$.

AST type checking: After expansion, ASDF type checks the AST. The ASDF type checker enforces linear types for qubits: any quantum value must be used exactly once and cannot be discarded [2, 35, 43, 64]. Type checking also verifies that functions marked as reversible call only other reversible functions and have no classical conditional expressions [2, 48, 53]. The most novel parts of the ASDF type checker involve validation of bases and basis translations. For example, the compiler must verify that each basis literal truly represents an orthonormal basis by checking the conditions on basis literals enumerated in Section 2.2. Type checking for a basis translation is more involved, as described below.

4.1 Span Equivalence Checking

A basis translation $b_{\text{in}} \gg b_{\text{out}}$ passes type checking if b_{in} and b_{out} pass type checking and $\text{span}(b_{\text{in}}) = \text{span}(b_{\text{out}})$, that is, if both (valid) bases span exactly the same subspace of qubit states [2, §A.2]. Henceforth, we call the problem of determining that $\text{span}(b_{\text{in}}) = \text{span}(b_{\text{out}})$ *span equivalence checking*. Span equivalence checking must be performed carefully because even simple bases in Qwerty may be exponentially large. For example, both $\{ '0', '1' \}[64]$ and $\{ '11', '0' \}[64]$ both represent 2^{64} basis vectors, meaning a naïve algorithm could require $O(2^{64})$ time to type check $\{ '0', '1' \}[64] \gg \{ '11', '0' \}[64]$. Instead, ASDF checks span equivalence in polynomial time.

The key insight in efficient span checking is using factoring — the opposite of the naïve approach of taking products of lists of vectors. Factoring appeals to the definition of tensor product [4, 34], by which $\{ \text{pre}_1, \text{pre}_2, \dots, \text{pre}_n \} + \{ \text{suff}_1, \text{suff}_2, \dots, \text{suff}_m \}$ is equal to the following basis:

$$\begin{aligned} & \{ \text{pre}_1 + \text{suff}_1, \text{pre}_1 + \text{suff}_2, \dots, \text{pre}_1 + \text{suff}_m, \\ & \text{pre}_2 + \text{suff}_1, \text{pre}_2 + \text{suff}_2, \dots, \text{pre}_2 + \text{suff}_m, \\ & \dots, \\ & \text{pre}_n + \text{suff}_1, \text{pre}_n + \text{suff}_2, \dots, \text{pre}_n + \text{suff}_m \} \end{aligned}$$

Factoring recovers the first form given the second form.

ASDF performs span equivalence checking with two queues of basis elements, one queue for each side of the basis translation. At each iteration, a basis element is popped from each queue, factoring the larger of the two if their dimensions do not match. After factoring, both basis elements at each iteration must either be identical or both fully span. (The check for equality holds because b_{in} and b_{out} are initially *normalized* — vector phases are removed and basis vectors are sorted lexicographically.) The efficient span checking algorithm runs in time $O(k^2 \log k)$, where k is the number of AST nodes making up the basis translation. Full details of the factoring algorithm, including a proof of its time complexity, can be found in Appendix B.

Example: Fig. 3 shows an example of type checking the basis translation written on the first two lines of the figure. The blue circles at each step represent the heads of the queues of basis elements. Note that each rewrite shown does not necessarily represent a semantically identical basis translation; rather, each step guarantees only that the span of each side of the translation is unchanged.

4.2 AST Canonicalization

After typechecking guarantees that the AST is well-formed, ASDF canonicalizes the AST, performing rewrites such as the following:

- **Removing** double-adjointing (i.e., replacing $\sim\sim f$ with f);
- **Rewriting** $\text{std}[N] \ \& \ f$ to $\text{id}[N] + f$ (because $\text{std}[N]$ fully spans);
- **Substituting** $\sim(\mathbf{b}_1 \gg \mathbf{b}_2)$ with $\mathbf{b}_2 \gg \mathbf{b}_1$;
- **Replacing** $\mathbf{b}_3 \ \& \ (\mathbf{b}_1 \gg \mathbf{b}_2)$ with $\mathbf{b}_3 + \mathbf{b}_1 \gg \mathbf{b}_3 + \mathbf{b}_2$; and
- Performing *float constant folding*.

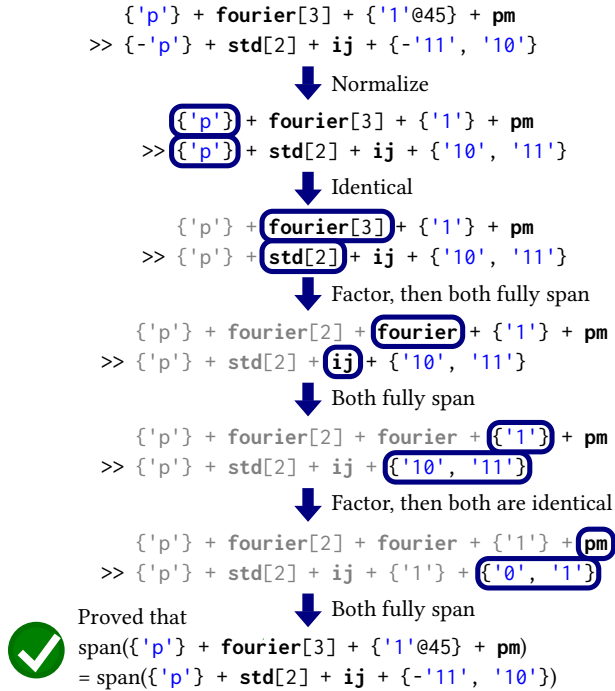


Figure 3. An example of how ASDF type checks a Qwerty basis translation.

AST optimizations simplify the IR produced, making the output amenable to subsequent IR-level optimizations. Additionally, optimizations require less engineering when done at the AST level — inside the compiler implementation, most of these optimizations are ~5 lines of code at the AST level versus ~50 lines at the MLIR level.

5 Qwerty IR

After ASDF performs type checking, little other compilation can happen at the AST level — a more structured representation is needed. For instance, while the semantics of Qwerty code can be gleaned from the AST, one cannot easily reason about dependencies between operations from the AST alone. The mission of the Qwerty MLIR dialect (or *Qwerty IR*) is to represent these dependencies while faithfully preserving language semantics.

Qwerty IR is a quantum SSA (static single assignment) IR whose structure is inspired by prior gate-level IRs such as QIRO and QSSA [23, 36]. Quantum instructions do not have side effects; instead, qubits flow through operations (e.g., basis translation operations), causing dependencies to be explicit in the IR. This naturally aligns with the linear qubit type in Qwerty [2] and allows for optimizations and lowering via simple DAG-to-DAG rewriting.

Qwerty IR Types: Qwerty IR defines three types: a tuple of N qubits, written **qbundle**[N]; a tuple of N bits, written **bitbundle**[N]; and a function type which may be either reversible or irreversible. By nature of MLIR allowing mixing

operations from multiple dialects, Qwerty IR may contain types from other dialects, such as the **qubit** type from the QCircuit MLIR dialect (Section 6) or the **f64** or **i1** types built into MLIR.

Qwerty IR Attributes: The most pivotal compile-time constant values (i.e., MLIR attributes) in Qwerty IR are those used to represent the structure of bases: **BuiltinBasis**, **BasisVector**, **BasisLiteral**, and **Basis**. These attributes respectively correspond to the definitions of built-in basis, basis vector, basis literal, and a canon form of a basis as defined in Section 2.2. For example, **pm**[2] + {'p'} in Qwerty code corresponds to a **Basis** with two elements: (1) a **BuiltinBasis** with primitive basis **pm** and dimension 2, and (2) a **BasisLiteral** containing only one **BasisVector** with primitive basis **pm** and eigenbits 0.

Qwerty IR Operations: The following are the key quantum operations in Qwerty IR:

- **qbprep** std<PLUS>[3], which prepares a qbundle in the given primitive basis and eigenstate ($|000\rangle$ in this example);
- **qbdiscard** %qb, which resets each qubit in the bundle %qb and returns the qubits to the ancilla pool;
- **qbdiscardz** %qb, which assumes the qubits are $|0\rangle$ and returns them to the ancilla pool without a reset;
- **qbtrans** %qb by b1 >> b2, which performs the basis translation b1 >> b2 on the qbundle %qb, returning a new qbundle; and
- **qbmeas** %qb in b, which measures the qbundle %qb in the basis b.

There are also structural operations such as **qbpack**, **bitpack**, **qbunpack**, and **bitunpack**, all of which create or destructure qbundles and bitbundles. To support adjoining and predicating functions, respectively, Qwerty IR contains ops such as **func_adj** %f and **func_pred** b %f, where %f is a function value and b is a basis. A direct call op may also be marked as an adjoint or predicated call, as in **call adj** @f() or **call pred**(b) @f(). There is also an indirect call op that calls a function value, **call_indirect** %f().

5.1 Lowering a Qwerty AST to Qwerty IR

With Qwerty IR now defined, we turn to the necessary compilation step of converting a Qwerty AST to Qwerty IR. Producing Qwerty IR from a Qwerty AST is straightforward overall, but the AST and IR have some structural differences. First, the AST has a tensor product node, but Qwerty IR does not have a tensor product op. This is handled differently depending on the types being tensored together: qbundles are both **qbunpacked** and then repacked with **qbpack** into a combined qbundle; **BasisAttrs** have their lists of basis elements concatenated; and functions are tensored by generating a **lambda** op that unpacks the input qbundle, calls both functions with repacked arguments, unpacks the result of each, and then returns a repacked combined qbundle.

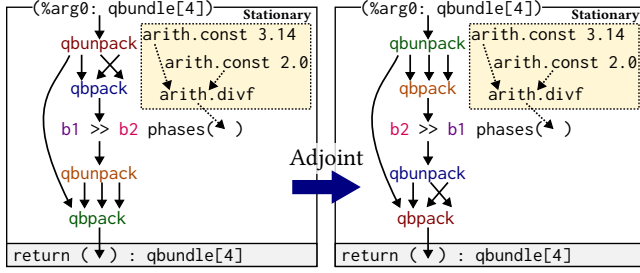


Figure 4. An example of adjoining a basic block

Another major difference between the AST and IR is that $b1 \gg b2$ in Qwerty is a function value, whereas $qbtrans$ in Qwerty IR is merely an op. Program semantics are preserved by wrapping the $qbtrans$ in a λ . The process for lowering other Qwerty built-in functions like $b.measure$ for some basis b is similar [2]. In general, the initial Qwerty IR produced by the AST walk will never contain $call$ ops, only $call_indirect$ ops, since the Qwerty pipe operator $|$ found in the AST calls function values, not symbol names.

5.2 Taking the Adjoint of Basic Blocks

Although Qwerty IR can express a $call\ adj\ @f(\%qb)$, we do not assume hardware has the capability to run code backwards. Instead, ASDF can take the adjoint of a function. This is done similarly to the Catalyst compiler [22], except that the algorithm for adjoining a basic block in ASDF is not hardcoded for particular ops. Instead, adjointable ops implement the Adjointable op interface, which includes a method `buildAdjoint()` that builds an adjoint form of a particular op. This way, the Qwerty compiler can traverse the def-use DAG in a basic block backwards from the block terminator, calling `buildAdjoint()` on each op encountered to rebuild a reversed form top-down. Classical operations, such as `arith.const` ops that define `f64` phase angles, complicate this process because such classical logic may not be reversible. We call such operations *stationary* because they remain in-place even if the rest of the DAG (the quantum portion) is inverted around them. In Fig. 4, for example, the classical `arith` ops in the yellow box are not adjointed.

5.3 Predicating Basic Blocks

Fortunately, predicating a basic block as needed by a $call\ pred(b)\ @f(\%qb)$ does not require inverting the def-use DAG. In most cases, in fact, predication means rebuilding block operations in-place with new predicates present (e.g., adding the $\{ '111' \}$ basis element to both sides of the basis translation in Fig. 5). This is accomplished with a Predicable op interface that includes a `buildPredicated()` method. While adding predicates to all non-stationary ops is necessary, per-op predication is not enough to guarantee the block does not modify states that are orthogonal to the predicate. This is because the dataflow semantics of

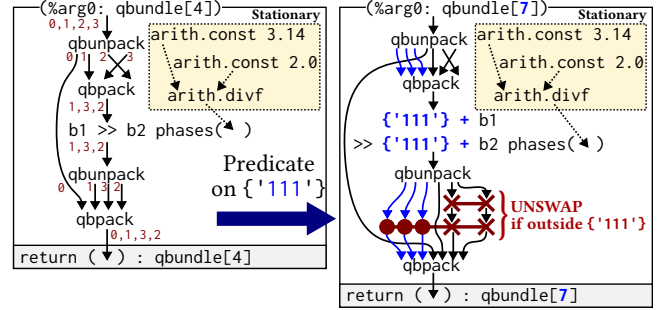


Figure 5. An example of predicating a basic block. The red gates shown on the right are SWAP gates; the second has three controls.

Qwerty IR allows effective swaps of qubits using renaming. In the unpredicated block on the left of Fig. 5, for example, the rightmost two qubits in the four-dimensional qbundle are swapped by renaming, and this renaming will occur regardless of the new predicates on the subsequent basis translation.

Undoing swaps in orthogonal spaces: As the final step of predicating a basic block, logical swaps achieved by renaming must be identified, and cleanup code must be inserted to undo each swap in the space orthogonal to the predicate. To accomplish this, ASDF runs an intraprocedural dataflow analysis that maps each MLIR value of type qubit or qbundle to a list of qubit indices that the value represents. The unpredicated block in Fig. 5 shows an example of these indices drawn in red on each non-stationary value edge. The analysis begins by assigning fresh indices to each non-stationary argument to the basic block. These indices are then propagated across the def-use chains in the basic block. When the analysis completes, the permutation effected by the unpredicated block is decomposed into a series of swaps. This sequence of swaps is reversed so that the permutation is undone, and then two SWAP gates are emitted for each: one uncontrolled SWAP to unconditionally undo the logical swap across the whole state space, and a second predicated SWAP to redo the swap inside the predicated space. (This is a trick to undo the original renaming-based swap inside the space orthogonal to the predicate.)

An example of this swap-unswap gate sequence is shown in red in the bottom right of Fig. 5. Observe that when the leftmost three qubits are $|111\rangle$, the two red SWAP gates in Fig. 5 will cancel out, leaving the rightmost two qubits swapped by renaming as desired. If the predicate qubits are in a different computational basis state such as $|101\rangle$ (i.e., the function runs on a state orthogonal to the predicate), the second (controlled) SWAP gate will not execute, making the first SWAP gate cancel out the initial swap achieved by renaming.

5.4 Qwerty IR Optimizations

To target the broadest set of quantum hardware, it is desirable to convert functional Qwerty code into a straight-line sequence of quantum operations if possible. To this end, inlining is the most important optimization in the Qwerty compiler. However, despite `call_indirect` ops mirroring Qwerty semantics, indirect calls are more clumsy to inline, so it is desirable to replace as many `call_indirects` as possible with direct `calls` instead. This can be challenging in the presence of `lambdas`, which cannot be directly converted to `calls` because they have no symbol name to reference.

The compiler overcomes the brunt of these issues with the following sequence of passes: (1) lifting all `lambdas` to `funcs` referenced by `func_consts`; (2) running the MLIR canonicalizer, which we configure to convert every instance of `call_indirect(func_const @f)()` into `call @f()`; and (3) running the MLIR inliner, which repeatedly inlines and re-runs the canonicalizer to find new inlining opportunities. This canonicalization includes patterns in the IR involving `func_adj` or `func_pred`, such as `call_indirect(func_pred {'10'} (func_adj (func_const @f)))()`, which becomes `call adj pred({'10'}) @f()`. When calls with `adj` or `pred` are inlined, the routines in Sections 5.2 and 5.3 are used to transform the single basic block making up the callee function body. Despite the general effectiveness of this approach, some Qwerty code can still produce IR that is tricky to inline, which we mitigate with specialized canonicalization patterns. One such inlining-enabling pattern pushes `call_indirect` ops whose callee is defined by an `scf.if` op upward into both forks of the `scf.if` op (see Appendix C for details).

6 QCircuit Dataflow IR

While the high-level semantics of Qwerty IR are valuable for analysis or transformations at that abstract level, directly lowering Qwerty IR to an output format such as QIR would be quite tedious and likely suboptimal. ASDF fills the gap between Qwerty IR and an optimized output circuit using another level of IR: the QCircuit MLIR dialect (or *QCircuit IR*), a gate-level dataflow-semantics quantum IR similar to QIRO or QSSA [23, 36]. It takes particular inspiration from McCaskey and Nguyen’s MLIR dialect [29], which also acts as a sort of MLIR dialect for QIR.

QCircuit IR Types: QCircuit IR has three types: `qubit`, `array<T>[N]`, and `callable`. These types correspond to the `%Qubit*`, `%Array*`, and `%Callable*` types in QIR.

QCircuit IR Operations: The core operations in QCircuit IR are the following:

- `qalloc`, which allocates a qubit;
- `qfree %q`, which frees a qubit;
- `qfreez %q`, which is similar to `qfree` but assumes the qubit is $|0\rangle$ and skips the reset performed by `qfree`;

- `measure %q`, which measures a qubit in the standard basis, yielding the new state and an `i1` result; and
- `gate G [%c1, ..., %cM] %q1, ..., %qN`, which runs a controlled `G` gate, taking `M+N` qubits and yielding their new states. The operands in square brackets `[.]` are controls and the rest are targets.

The structural `arrpack` and `arrunpack` ops facilitate code that manipulates arrays, being analogous to the `qbpack` and `qbunpack` ops for qbundles in Qwerty IR. To support callable values, QCircuit IR includes ops for holding callable value metadata and for invoking, controlling, or adjointing `callables`; these correspond closely to both the function ops in Qwerty IR and to QIR callable intrinsics [20]. Thanks to canonicalization and inlining (Section 5.4), ops for arrays and callables are rarely used in realistic QCircuit-dialect IR generated by the ASDF compiler. To our knowledge, though, ASDF is the first MLIR-based compiler to generate QIR callables [20].

6.1 Lowering Qwerty IR to QCircuit IR

Conversion from Qwerty IR to QCircuit IR is performed using the MLIR dialect conversion framework [26], in which conversions are defined using rewrite patterns. For example, we define a conversion pattern to decompose the Qwerty `qbdiscard` op into a `qbunpack` that feeds into N QCircuit-dialect `qfree` ops. (The Qwerty `qbunpack` is then converted into a QCircuit `arrunpack`.) Lowering `qbprep` ops is similarly simple, with them being broken into N `qallocs` followed by `gate` ops for H , S , and X gates, all of whose results are `qpacked` into the substituted result. A canonicalization pattern later removes redundant instances of `arrunpack(arrpack)` and `arrpack(arrunpack)`, usually leaving a clean DAG starting with `qallocs` and ending in `qfrees`. Lowering Qwerty IR in its full generality only becomes challenging when inlining fails or if programmers write nontrivial basis translations. We cover these issues in Sections 6.2 and 6.3. Section 6.4 then describes how ASDF uses Tweedledum to synthesize QCircuit dialect code from classical circuit descriptions [40]. Section 6.5 concludes by describing optimizations we perform in the QCircuit dialect.

6.2 Producing Function Specializations

One challenge in lowering Qwerty IR to QCircuit IR is that a function value in Qwerty IR cannot be represented by a typical function pointer — i.e., a mere address of code in memory — in QCircuit IR. This is because a function value `%f` in Qwerty IR can be adjointed with `func_adj %f` or predicated on a basis `b` with `func_pred b %f`, each producing a new function value with fundamentally different structure. Thus, the compiler may need to generate multiple *specializations* of a given function to satisfy these requests [54].

Function specialization analysis: The most naïve conservative generation of all specializations for all functions is

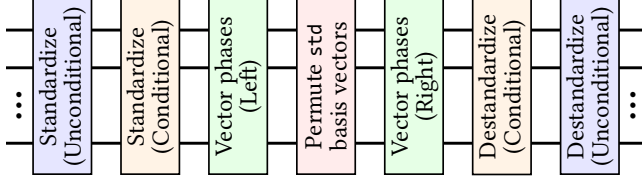


Figure 6. A summary of the structure of the circuit synthesized by ASDF for a basis translation (read left to right)

intractable because there are an enormous number of possible predicated specializations given different predicates. To avoid this, we run interprocedural dataflow analysis [39] on the IR to label each callable value with a set of tuples (funcName, isAdjoint, numControls). Then, the analysis for the callee operand can be checked at every **call_indirect** op, determining (along with every **call** op) the specializations of other functions that a forward (non-**adj** and non-**pred**) invocation of each function requires.

Transitive specialized calls: However, this analysis does not account for all paths through the call graph; specifically, by considering the callees of only a forward invocation of each function, it does not consider transitive specialization requirements. Consider the following IR, for instance:

```
func f() {
    call adj g(...)
}
func g() {
    call h(...)
}
func h() {
    ...
}
```

An adjoint specialization of $h()$ is needed because the adjoint form of $g()$ is called by $f()$. However, this would not be detected by the initial analysis because there is no explicit **call adj** $h()$ in the IR. ASDF addresses this problem by constructing a call graph of specializations and iteratively adding transitive edges as required. (See Appendix D for the full algorithm.)

6.3 Lowering Basis Translations to Gates

The toughest challenge in lowering Qwerty IR to QCircuit IR is synthesizing the quantum gates that achieve a basis translation. This is the most novel part of ASDF, in fact, as we are not aware of prior compilers that synthesize basis translations, only implementations that do more general (and more expensive) unitary synthesis [44].

As seen in Fig. 6, the core of a basis translation is a permutation of **std** basis vectors. Yet because the left-hand side of a basis translation can be defined in terms of non-**std** primitive bases, standardization runs first to translate qubits from that primitive basis to **std**. (Destandardization, which runs last, translates from **std** to the primitive basis on the right-hand side of the goal translation.) The phases that programmers supply for basis vectors are handled between the steps of (de)standardizing and permutation since a typical gateset makes imparting phases most convenient in the standard basis. The following sections describe the steps in synthesis. **Standardization:** Performing standardization for a basis

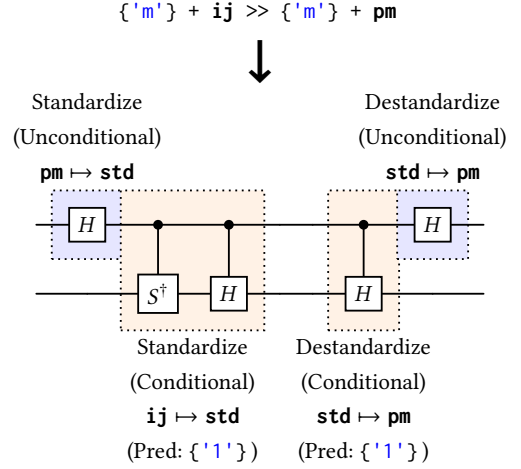


Figure 7. An example of basis translation circuit synthesis by ASDF involving both conditional and unconditional standardization

translation $b_{in} \gg b_{out}$ begins by collecting two lists of pairs (prim, dim), where prim is a primitive basis and dim is the number of qubits, one list for b_{in} and the other for b_{out} . These lists represent the ranges of primitive bases across basis elements of b_{in} and b_{out} , respectively, and the first is a list of *necessary standardizations* while the second is a list of *necessary destandardizations*. The former list specifies how primitive bases in b_{in} must be translated to **std** for all operand qubits at the beginning of synthesis, and the latter list specifies how **std** must be translated to the primitive bases in b_{out} at the end of synthesis. Each necessary (de)standardization is annotated as either *unconditional* or *conditional*, indicating whether it is present in both the list of necessary standardizations and destandardizations, i.e., both sides of the goal translation. Unconditional standardizations represent an unchanged primitive basis on either side of the translation, whereas conditional (de)standardizations represent a change in primitive basis.

The distinction between conditional and unconditional (de)standardization matters when a basis translation has predicates. The gates that perform unconditional standardization do not need to be controlled such that they run only in the space on which the goal translation is predicated, since unconditional standardizations will be undone by their corresponding destandardizations. (In quantum parlance, the rest of the synthesized circuit is *conjugated* by unconditional (de)standardizations.) For instance, if the upper qubit in Fig. 7 is initially $|+\rangle$, the controlled gates shown will not run and the H gates on the upper qubit will cancel out, leaving the state correctly unaffected. On the other hand, the controlled gates in Fig. 7, which achieve a conditional standardization, could not be replaced with uncontrolled gates because the circuit would incorrectly modify the input state

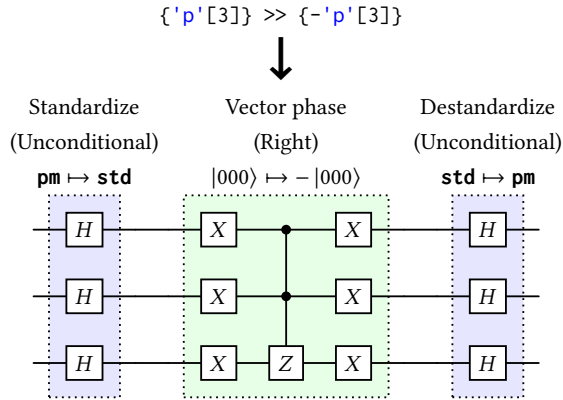


Figure 8. An example of basis translation circuit synthesis involving an vector phase

if the upper qubit is e.g. $|+\rangle \notin \text{span}(|-\rangle)$. (In general, the erroneous circuit would behave as $\{ 'p', 'm' \} + \mathbf{ij} \gg \{ 'p', 'm' \} + \mathbf{pm}$ instead of the goal translation shown in Fig. 7.) The full process of determining which (de)standardizations are conditional is shown in Algorithm E6 in Appendix E.

Once (de)standardizations and their conditionality are determined, implementing unconditional standardizations is straightforward using H and S gates (for \mathbf{pm} and \mathbf{ij}) or N -bit IQFT (inverse quantum Fourier transform, for $\mathbf{fourier}[N]$). Unconditional destandardization is simply the adjoint of these operations. Synthesizing conditional (de)standardizations requires controlled forms of these, yet in typical gate-sets, controlling on $|0\rangle$ and $|1\rangle$ is more convenient than controlling on vectors in other primitive bases. Fortunately, span equivalence checking (Section 4.1) guarantees that all predicates in a well-typed basis translation correspond to unconditional standardizations. Thus, ASDF synthesizes an outer layer of unconditional (de)standardizations before synthesizing an inner layer of controlled conditional (de)standardizations, as seen in Fig. 7.

Vector Phases: Given the goal basis translation $b_{\text{in}} \gg b_{\text{out}}$, the compiler scans each of b_{in} and b_{out} for basis vectors with phases. The result is two lists of tuples (eigenbits, θ , offset), one list for the input basis b_{in} and one for the output basis b_{out} . As shown in Fig. 6, after standardization, the input state is translated from \mathbf{std} with the input phases to \mathbf{std} without phases. Then any desired phases are re-introduced before destandardization via translation from \mathbf{std} to \mathbf{std} with the output phases. These translations are achieved with X -conjugated multi-controlled- $P(\theta)$ gates. Fig. 8 shows an example of synthesizing a translation that uses vector phases to implement a three-qubit Grover diffuser [17, 18, 34].

Permutation: With standardization and vector phases handled, only the center of Fig. 6 remains: synthesizing a circuit that implements the reversible classical function $f : \mathbb{B}^n \rightarrow \mathbb{B}^n$, which acts as a permutation on $\mathbf{std}[n]$ basis vectors.

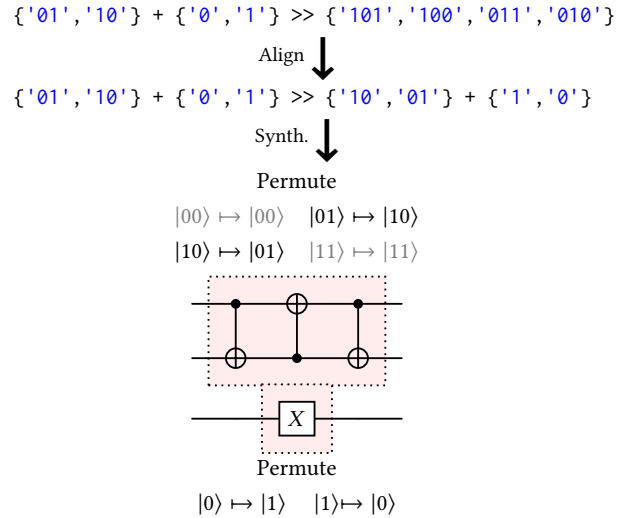


Figure 9. An example of basis translation circuit synthesis involving a permutation

Unless the permutation is the identity, this synthesis is performed for each pair of respective basis elements in the two bases. (If respective bases elements are different dimension and thus do not operate on the same qubits, a factoring-based process of *alignment* is necessary. This is discussed in detail in Appendix F.) In Fig. 9, for instance, synthesis runs twice: once for the permutation defined for the first two qubits and again for the permutation defined for the last qubit. Presently, ASDF uses the multidirectional transformation-based synthesis algorithm [33, 50] implemented in the Tweedledum library [40]. Controls are added to the Tweedledum-generated circuit as necessary to obey the predicates in aligned bases.

6.4 Synthesizing Classical Functions

Basis-oriented constructs are not the only way that Qwerty programmers can express program code, since Qwerty also supports synthesizing circuits from classical logic [2]. The `@classical` function on lines 5-7 of Fig. 1 is an example of this feature. ASDF begins compiling `@classical` functions similarly as it does for `@qpu` functions (Section 4), by extracting a custom AST from the Python AST and performing type checking [13]. This AST is then converted to a classical logic network in the mockturtle library [52]. After running some classical optimizations provided by mockturtle, ASDF passes this classical circuit to tweedledum [40], which generates a Bennett embedding $U_f |x\rangle |y\rangle = |x\rangle |y \oplus f(x)\rangle$ for the corresponding classical function f [5, 31, 41]. The result is expressed in tweedledum Circuit IR, which we transpile to QCircuit IR. Inside a Qwerty `@qpu` function, the programmer can request this Bennett embedding for f with the syntax `f.xor`. The syntax `f.sign` generates the form $U'_f |x\rangle = (-1)^{f(x)} |x\rangle$ instead, which ASDF generates by passing $|-\rangle$ ancilla to the output of the Bennett embedding [34].

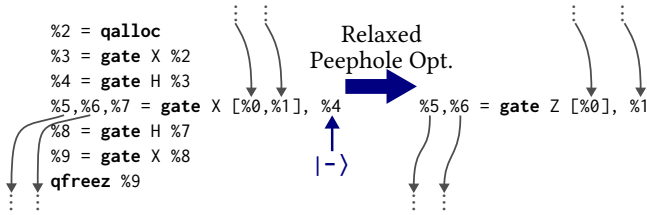


Figure 10. A relaxed peephole optimization performed on QCircuit-dialect IR

6.5 QCircuit IR Optimizations

Before generating the output circuit from QCircuit IR, we run optimizations to remove redundancies left behind by earlier systematic lowering. For instance, in Fig. 7, the adjacent controlled-Hadamards generated by basis translation circuit synthesis should cancel out. We implement similar common gate-level optimizations as those in prior work [23, 36], such as cancelling out adjacent Hermitian (self-adjoint) gates or replacing HXH with Z . We also implement some relaxed peephole optimizations due to Liu, Bello, and Zhou [27], including the one shown in Fig. 10, which turns a multi-controlled X with a $|-\rangle$ target into a multi-controlled Z without the $|-\rangle$ ancilla. This particular optimization is especially useful for simplifying instances of f . **sign** (used in Bernstein–Vazirani or Grover’s), which typically involves the situation shown in Fig. 10 (see Section 6.4). As a final optimization step, multi-controlled gates are decomposed using Selinger’s controlled- iX scheme to reduce T gate counts on fault-tolerant hardware [42].

7 Targeting OpenQASM 3 and QIR

Transpiling to OpenQASM 3: From QCircuit IR, ASDF can produce OpenQASM 3 [9] using a process akin to `reg2mem` in QSSA [36], in which SSA (static single assignment) values are converted to quantum register accesses. Because OpenQASM 3 does not support function pointers or qubit allocation inside subroutines, OpenQASM 3 generation is currently dependent on inlining succeeding (Section 5.4), although this has not empirically presented a problem for realistic Qwerty programs (see Section 8.2).

Producing QIR: ASDF produces QIR by using MLIR dialect conversion from the QCircuit MLIR dialect to the built-in MLIR dialect named `llvm`, which models LLVM IR [21, 25]. For the Unrestricted QIR profile (in which the full generality of QIR is allowed), this means individually converting each QCircuit op into calls to the corresponding QIR intrinsics. For example, `qalloc` becomes a call to `__quantum__rt__qubit_allocate()`, and a `gate` is converted to a call to the corresponding gate intrinsic. Callable-related ops are lowered to calls to equivalent callable intrinsics. ASDF-generated QIR requires only one change to the QIR runtime that amounts

to removing approximately 50 lines of Q#-specific runtime code (see Appendix G for details).

Targeting the QIR base profile: In contrast with the Unrestricted QIR profile, the QIR Base Profile is highly restricted [21], effectively amounting to a straight-line sequence of gates embedded in LLVM IR. In the Base Profile, there is no dynamic qubit allocation; instead, `%Qubit*`s passed to gate intrinsics are integral qubit indices casted to pointers. Thus, a similar `reg2mem` process as used in OpenQASM 3 export is used to insert the LLVM `inttoptr` casts that act as `qallocs` [36].

Execution: The Qwerty runtime included with ASDF is pre-configured to target either local simulation with `qir-runner` [58] or a variety of backends via QIR-EE [61], a convenient adaptor for executing QIR via XACC [30]. ASDF produces Unrestricted Profile QIR for `qir-runner` but Base Profile QIR for QIR-EE. (ASDF-generated QIR could also be sent to cloud services such as Azure Quantum provided that LLVM versions sufficiently align.)

8 Evaluation

To our knowledge, no other compilers for basis-oriented quantum programming languages exist, including Qwerty, so we evaluate ASDF by comparing it with compilers for circuit-oriented languages. First, in Section 8.2, we investigate the effectiveness of inlining in ASDF (Section 8.2) by comparing with a Q# compiler. Then, in Section 8.3, we compare the cost of Qwerty code versus circuit-oriented code in terms of metrics for fault-tolerant quantum hardware. (Note that the intention of ASDF is to synthesize circuits with similar performance to handwritten circuits, not to outperform handwritten circuits.)

8.1 Experimental Setup

Software packages used: We evaluate using Python 3.11.2, Qiskit 1.2.0, Quipper 0.9.0.0, Classic Q# QDK 0.27, Modern Q# QDK 1.6, LLVM 19.1.2, and Haskell 8.6.5. The `quipper-qasm` tool was used to convert Quipper code to OpenQASM [7]. We modified the Qiskit `-03` transpiler to remove a few particular passes that were causing nondeterminism in evaluation results. Before removal, these passes had a maximum of $<0.1\%$ positive performance impact, so the impact on our evaluation is negligible.

Benchmarks: We test with five popular quantum algorithms: Bernstein–Vazirani with an alternating secret string (1010...) [6, 12], Deutsch–Jozsa with a balanced oracle that XORs all input bits [11, 34], Grover’s search with an oracle matching the input consisting of all 1s [17, 18, 34], Simon’s algorithm with a nonzero secret string [46, 47], and QFT-based period finding with an oracle performing bitmasking [34]. All benchmarks are parameterized on the size of a classical input to their oracle. To make the evaluation feasible, the Grover’s benchmark is capped at 12 iterations. For all benchmarks,

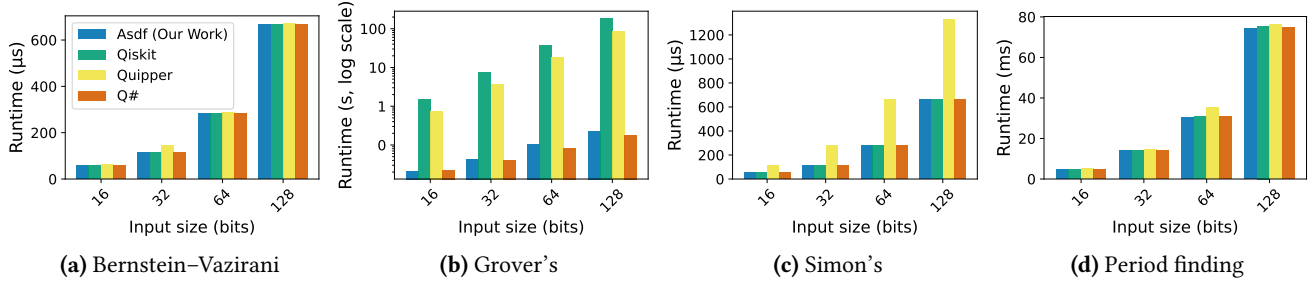


Figure 11. Runtime of benchmarks for each compiler for different oracle input sizes (lower is better)

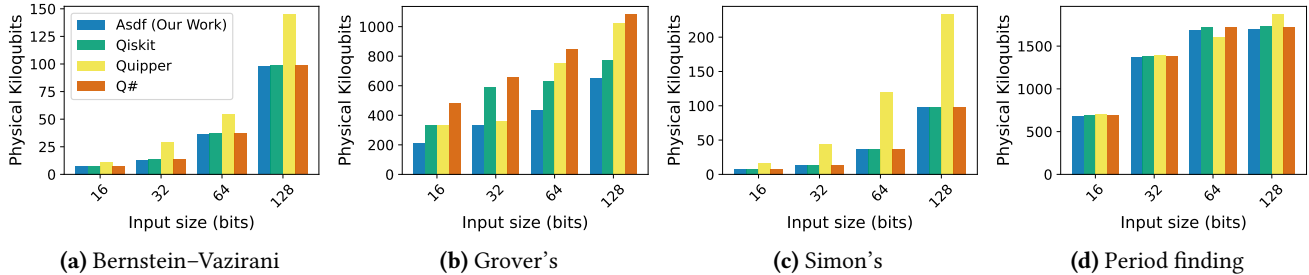


Figure 12. Physical qubits used by each benchmark by each compiler for different oracle input sizes (lower is better)

oracles are expressed as classical logic in both Quipper and Qwerty, but as gates in Qiskit and Q#. The Q# code is largely taken from Wojcieszyn [60]; the Qiskit implementations are derived from the original Qiskit textbook [62]; the Quipper implementations are inspired by Siddiqui et al. [45] and Green et al. [15]; and the Qwerty programs are derived from the examples by Adams et al. [2].

8.2 Impact of Inlining

If a compiler targets QIR, a good measure of its success in inlining is how many QIR callable intrinsics it emits. Presently, the QIR callables API is not well supported by hardware partners, so fewer calls to callables intrinsics is preferred. We compare ASDF with inlining enabled (Section 5.4), ASDF with inlining disabled, and the Classic Q# QDK. (We use the Classic Q# QDK rather than the Modern Q# QDK because at the time of writing, the Modern QDK cannot yet generate QIR callables.) Table 1 shows the results. The metrics shown on the “create” and “inv.” columns of Table 1 are the number of invocations of `__quantum__rt__callable_create` and `__quantum__rt__callable_invoke`, respectively, in the LLVM assembly (QIR) produced by the compiler. It is clear that ASDF is highly effective for realistic benchmarks at inlining Qwerty programs into a single QIR function suitable for the QIR Base Profile, but also that ASDF preserves soundness by still emitting callables when necessary (e.g., when inlining is disabled).

Table 1. QIR callable intrinsics generated by different compiler configurations.

	Q#		ASDF (No Opt)		ASDF (Opt)	
	create	inv.	create	inv.	create	inv.
B-V	5	8	3	3	0	0
D-J	4	4	2	2	0	0
Grover	6	4	5	16	0	0
Period	12	16	4	4	0	0
Simon	4	4	7	7	0	0

8.3 Comparison with Gate-Oriented Languages

In this section, we consider the overhead of writing common quantum programs in Qwerty and compiling with ASDF versus writing in traditional circuit-oriented languages and compiling with their respective compilers. Our methodology follows: (1) generate quantum assembly [9, 10] from all five benchmarks in all four languages for different oracle input sizes; (2) optimize the resulting code with the Qiskit transpiler set to `-03` [38]; and (3) feed the resulting optimized assembly into Azure Quantum Resource Estimator [57], which estimates **physical qubit count** and **runtime** for the circuit on fault-tolerant hardware. Both metrics are important because functionally equivalent circuit designs often face a tradeoff of qubit count versus runtime [14, 40]; increasing qubit count may make algorithms out of reach of hardware, yet a longer runtime may carry greater monetary cost and gives more opportunity for error to accumulate. We use the default estimation parameters, which model a [[338, 1, 13]]

surface code with a $5.2\ \mu\text{s}$ cycle time [57]. The Modern Q# QDK compiler was used to compile Q# [32].

Results are shown in Figs. 11 and 12. (Deutsch–Jozsa results, not shown, were virtually identical to Bernstein–Vazirani due to their similar circuit structure.) The circuits generated by ASDF consistently keep pace with circuit-oriented languages despite the Qwerty programs containing no hand-programmed gates. The Tweedledum-powered circuit synthesis in ASDF (Section 6.4) consistently matches or beats the performance of the oracle synthesis in the Quipper compiler, likely due to Quipper’s willingness to use ancilla qubits for XOR operations, which is intentionally avoided by the synthesis algorithm implemented in Tweedledum [41]. The Q# compiler and ASDF outperform other compilers significantly for Grover’s (Figs. 11b and 12b) due to using Selinger’s decomposition of multi-controlled gates (see Section 6.5) [42]. Note that small variations in performance, such as Quipper’s slight deviations from others in period finding (Figs. 11d and 12d) are caused by slightly differently circuit structure being marginally more or less favorable to the Qiskit transpiler — in this case, this difference is Quipper using renaming-based swaps for IQFT rather than SWAP gates.

These results show that even with Qwerty’s higher level of abstraction, ASDF enables Qwerty programs to perform similarly to handwritten quantum circuits.

9 Related Work

Quantum MLIR dialects: To our knowledge, operations in the Qwerty MLIR dialect (Section 5) can better signify programmer intent and program structure than most existing quantum MLIR dialects; for example, the op to prepare a primitive basis state (**qbprep**) is distinct from the basis translation op used for state evolution (**qbtrans**). Dialects such as QIRO or QSSA would likely represent both cases with low-level gate ops instead [23, 36]. Similarly, both CUDA-Q’s Quake dialect [55] and IBM’s QCS and QUIR consist of gates as the fundamental quantum operation on qubits [19]. In comparing levels of abstraction between the Qwerty MLIR dialect and prior quantum dialects, Xanadu’s quantum dialect in their Catalyst compiler is an exception, however. While the dialect mostly contains lower level gate operations, it does contain some higher abstraction operations, such as an operation dedicated to computing a Hamiltonian observation given an array of observables as input [22]. This is a higher level of abstraction than Qwerty reasons about, as it is specific to an application domain (quantum chemistry).

Quantum compilers: Prior quantum compilers have implemented similar features to our work, such as auto-generation of function specializations (Section 6.2) and synthesis of circuits from a classical description (Section 6.4). Q#, for example, allows writing `Adjoint f` and `Controlled f`, for a function value `f`, so Q# compilers can auto-synthesize the

specializations that these expressions request [53, 54]. However, Qwerty’s predication (`b & f`) is more general than a control in circuit-oriented programming. Additionally, the compilers for Scaffold, Quipper, and Q# can all automatically synthesize quantum circuits from classical circuits, which can then be used as oracles and subroutines in a programmer’s quantum program [1, 16, 24, 51].

10 Conclusion

Qwerty is a high-level quantum programming language designed around bases and functions instead of gates. This new quantum programming paradigm introduces new challenges in compilation, including synthesizing circuits and specializing adjoint or predicated forms of functions. This paper presented *ASDF*, a compiler that answers these challenges with a type system and a series of high and low-level optimization passes. *ASDF* uses a new, custom dialect of MLIR, *Qwerty IR*, which is capable of being lowered to a form ready for both simulation and execution on near-term hardware. In a comparison with the output of circuit-oriented compilers on hand-coded programs, *ASDF* has been shown to produce high-quality code across a set of well-known quantum algorithms. Future upgrades to *ASDF* should guarantee optimizations that are necessary for hardware targets with limited classical capability, such as inlining, and implement language features that support more physics-focused applications, such as Hamiltonian simulation.

Acknowledgments

The authors thank the anonymous reviewers and Pulkit Gupta for their helpful feedback. We acknowledge support for this work from NSF planning grant #2016666 and through the ORNL STAQCS project. Support for this work also came from the U.S. Department of Energy, Office of Science, Advanced Scientific Computing Research Accelerated Research in Quantum Computing Program under field work proposal ERKJ332. This research was supported in part through research infrastructure and services provided by the Rogues Gallery testbed [37, 63] hosted by the Center for Research into Novel Computing Hierarchies (CRNCH) at Georgia Tech. The Rogues Gallery testbed is primarily supported by the NSF under NSF Award Number #2016701.

A Artifact Appendix

A.1 Abstract

Our artifact contains quantum algorithm benchmarks (written in Q#, Quipper, Qiskit, and Qwerty), scripts for extracting resource estimates from these benchmarks, and the *ASDF* compiler and runtime for Qwerty. Only a Linux machine with Docker and sufficient memory (approximately 32 GB of RAM) is needed to run the evaluation.

A.2 Artifact check-list (meta-information)

- **Algorithm:** Quantum circuit synthesis
- **Program:** Custom benchmarks, included in artifact
- **Compilation:** gcc 11.4.0 and LLVM 19.1.2, both included in Docker image
- **Transformations:** Custom compiler passes, included in artifact
- **Binary:** x86_64 binaries for Linux (Ubuntu 22.04.5 LTS) packaged as Docker image
- **Metrics:** (1) number of calls to QIR intrinsics; (2) estimated physical qubits for a surface code; and (3) estimated runtime on a surface code
- **Output:** Table and graphs (Table 1 and Figs. 11-12, respectively)
- **Experiments:** The artifact README describes how to run experiments
- **How much disk space required (approximately)?:** Approximately 30 GB (evaluation results are only 50 MB, but both Docker images are 14 GB combined)
- **How much time is needed to prepare workflow (approximately)?:** Under 1 hour to download and load Docker images
- **How much time is needed to complete experiments (approximately)?:** Under 4 hours
- **Publicly available?:** Yes
- **Code licenses (if publicly available)?:** MIT license
- **Archived (provide DOI)?:** 10.5281/zenodo.14505385

A.3 Description

A.3.1 How delivered. The artifact is available on Zenodo at the following link: <https://doi.org/10.5281/zenodo.14505385>

A.3.2 Hardware dependencies. Sufficient memory, approximately 32 GB total. Approximately 30 GB of disk space.

A.3.3 Software dependencies. Docker on Linux.

A.4 Installation

Run the following two commands:

```
docker image load -i \
  qwerty-artifact-docker.tar.xz
docker image load -i \
  qwerty-artifact-quipper-docker.tar.xz
```

A.5 Experiment workflow

The following command will compile Quipper programs to quantum assembly (this is done separately because Quipper requires a specific system configuration and thus its own Docker image):

```
mkdir data
docker run --rm -v $(pwd)/data:/data/ \
  qwerty-artifact-quipper quipper-bench-qasm.sh
```

(The generated assembly can be found on the host at `data/quipper/*.qasm`.)

The following command will run the evaluation pipeline:

```
docker run --rm -v $(pwd)/data:/data/ \
  qwerty-artifact eval/run-eval.sh
```

Afterward, `data/summary/` on the host contains a summary of the results of the evaluation.

Detailed results are found in other subdirectories of `data/`: the statistics for QIR callables for Q# versus Qwerty (Section 8.2) can be found in `data/count-callables/`, and detailed resource estimation (Section 8.3) results are in `data/compare-circs/`.

A.6 Evaluation and expected result

Table 1 should match `data/summary/table.csv` exactly. Fig. 11 should match `data/summary/time_*.pdf`. Fig. 12 should match `data/summary/physical_*.pdf`.

A.7 Notes

The full ASDF source code is included in the artifact as `qwerty-artifact-source.tar.xz`. (This code is also available at `/qwerty/` in the `qwerty-artifact` Docker image.) Inside the source tarball (or at `/qwerty/` in the Docker image), `README.md` explains how to build the compiler from source. Other files in `docs/` document the code structure, testing, debugging, evaluation, and integration with other tools.

B Span Checking Details

The efficient span equivalence checking algorithm described in Section 4.1 is written as pseudocode in Algorithm B1. The algorithm proves span equivalence using case analysis; its correctness can be proved inductively using a similar proof by cases. Algorithm B2 elaborates on sub-cases of the factoring performed on line 14 of Algorithm B1. Lines 1-5 of Algorithm B2 hold because of Lemmas B.1 and B.2. (Below, \mathcal{H}_2 denotes the single-qubit Hilbert space $\text{span}(|0\rangle, |1\rangle)$.)

Lemma B.1. $\text{span}(\text{fourier}[N]) = \text{span}(\text{fourier}[N_1]) \otimes \text{span}(\text{fourier}[N_2])$ if $N = N_1 + N_2$ and $N_1, N_2 \in \mathbb{Z}^+$.

Proof. Follows from $\mathcal{H}_2^{\otimes N_1+N_2} = \mathcal{H}_2^{\otimes N_1} \otimes \mathcal{H}_2^{\otimes N_2}$. \square

Lemma B.2. $\text{span}(\text{fourier}[N]) = \text{span}(\text{std}[N]) = \text{span}(\text{pm}[N]) = \text{span}(\text{ij}[N]) = \text{span}(\{bv_1, bv_2, \dots, bv_m\})$ if the basis literal is well-typed, fully spans, and has dimension $N \in \mathbb{Z}^+$.

Proof. All spans are $\mathcal{H}_2^{\otimes N}$. \square

The remaining cases, lines 6-13 of Algorithm B2, hold due to Lemma B.3:

Lemma B.3. *There exist bv'_j such that*

$$\{bv_1, bv_2, \dots, bv_{m_1}\} = \left\{ \left(\left(bv_{(k)} bv'_j \right)_{j=1}^{m_2} \right)_{k=0}^{2^n-1} \right\}$$

Input: A basis translation $b_{in} \gg b_{out}$
Output: Either success or failure

```

1 ldeque ← elements of  $b_{in}$ , each normalized
2 rdeque ← elements of  $b_{out}$ , each normalized
3 while ldeque and rdeque are not empty do
4    $\ell$  ← pop front of ldeque
5    $r$  ← pop front of rdeque
6   if dim  $\ell$  = dim  $r$  then
7     if  $\ell = r$ , or  $\ell$  and  $r$  both fully span then
8       continue
9     else
10      return failure
11  else
12    big ← max( $\ell, r$ )
13    small ← min( $\ell, r$ )
14    if factoring small from big fails
15      (Algorithm B2) then
16        return failure
17    else
18      continue
19 if either ldeque or rdeque is not empty then
20   return failure // Dimension mismatch
21 return success

```

Algorithm B1: Span equivalence checking for a basis translation.

Input: Two basis elements, big and small, and the deque for big from Algorithm B1 (bigdeque)
Output: Either success or failure

```

1 if both big and small fully span then
2    $\delta$  ← (dim big) – (dim small)
3   prim ← primitive basis of big
4   Push prim[ $\delta$ ] to front of bigdeque
5   return success
6 else if small fully spans and big is a basis literal
7   then
8     if factoring succeeds (Algorithm B3) then
9       Push remainder to front of bigdeque
10      return success
11 else if both small and big are basis literals then
12   if factoring succeeds (Algorithm B4) then
13     Push remainder to front of bigdeque
14     return success
15 return failure // Fallthrough

```

Algorithm B2: Factoring a basis element in span checking.

Input: A basis literal $bl = \{bv_1, bv_2, \dots, bv_m\}$ (with bv_i sorted lexicographically) and a positive integer n such that $(\dim bl) > n$
Output: Either success (and a remainder) or failure

```

1 if  $m$  is not divisible by  $2^n$  then
2   return failure
3 Count distinct  $n$ -bit prefixes across all  $bv_i$ 
4 if there are less than  $2^n$  distinct prefixes then
5   return failure
6 Count occurrences of  $(\dim bl - n)$ -bit suffixes across
  all  $bv_i$ 
7 if any suffix appears less than  $2^n$  times then
8   return failure
9 return success and distinct suffixes // Remainder

```

Algorithm B3: Factoring $\mathbf{std}[n]$, $\mathbf{pm}[n]$, or $\mathbf{ij}[n]$ from a basis literal bl in span checking. Bit operations are on eigenbits.

Input: Basis literals $bl = \{bv_1, bv_2, \dots, bv_m\}$ and $bl' = \{bv'_1, bv'_2, \dots, bv'_{m'}\}$, both sorted lexicographically and with $(\dim bl) > (\dim bl')$
Output: Either success (and a remainder) or failure

```

1 if  $bl$  and  $bl'$  have different primitive bases then
2   return failure
3 if  $m$  is not divisible by  $m'$  then
4   return failure
5  $n$  ← dim  $bl'$ 
6 Count distinct  $n$ -bit prefixes across all  $bv_i$ 
7 if there are less than  $m'$  distinct prefixes, or any prefix
  is not equal to some  $bv'_i$  then
8   return failure
9 Count occurrences of  $(\dim bl - n)$ -bit suffixes across
  all  $bv_i$ 
10 if any suffix appears less than  $m'$  times then
11   return failure
12 return success and distinct suffixes // Remainder

```

Algorithm B4: Factoring a basis literal bl' from a basis literal bl in span checking. Bit operations are on eigenbits.

if and only if

$$\begin{aligned} & \text{span}(\{bv_1, bv_2, \dots, bv_{m_1}\}) \\ &= \mathcal{H}_2^{\otimes n} \otimes \text{span}(\{bv'_1, bv'_2, \dots, bv'_{m_2}\}). \end{aligned}$$

(The notation $(\cdot)_i$ denotes the existence of some ordering of a comma-separated list. $bv_{(k)}$ represents a basis vector with the same primitive basis as all bv_i and eigenbits corresponding to the n -bit binary representation of k .)

Proof.

(\rightarrow): Definition of the tensor product on vector spaces.

(\leftarrow): Similar. \square

Algorithm B3, used on line 7 of Algorithm B2, implements Lemma B.3. It uses the following corollary as a short-circuit optimization (line 1 of Algorithm B3):

Corollary B.4. *If 2^n does not divide m_1 , then there are no bv'_j such that*

$$\begin{aligned} & \text{span}(\{bv_1, bv_2, \dots, bv_{m_1}\}) \\ &= \mathcal{H}_2^{\otimes n} \otimes \text{span}(\{bv'_1, bv'_2, \dots, bv'_{m_2}\}). \end{aligned}$$

Proof. (By contraposition) Suppose there exist bv'_j such that

$$\begin{aligned} & \text{span}(\{bv_1, bv_2, \dots, bv_{m_1}\}) \\ &= \mathcal{H}_2^{\otimes n} \otimes \text{span}(\{bv'_1, bv'_2, \dots, bv'_{m_2}\}). \end{aligned}$$

By Lemma B.3,

$$\{bv_1, bv_2, \dots, bv_{m_1}\} = \left\{ \left((bv_{(k)} bv'_j)_{j=1}^{m_2} \right)_{k=0}^{2^n-1} \right\}.$$

Clearly,

$$\left| \left\{ \left((bv_{(k)} bv'_j)_{j=1}^{m_2} \right)_{k=0}^{2^n-1} \right\} \right| = 2^n \times m_2.$$

Thus, $2^n \times m_2 = m_1$, i.e., m_1 is a multiple of 2^n . \square

Algorithm B4 appeals to a straightforward generalization of Lemma B.3 and Corollary B.4 (Algorithm B3) to factor out an arbitrary basis literal rather than only a fully-spanning basis. This requires some additional checks, namely lines 1 and 7 of Algorithm B4.

Lemma B.5. *Algorithms B3 and B4 run in time $O(k \log k)$ if k is the total number of AST nodes in the inputs.*

Proof. In Algorithm B3, bl can be sorted twice, first by prefixes and second by suffixes, to perform the counting needed. Algorithm B4 is similar: bl' can be sorted as well and binary searched to detect unexpected prefixes. \square

Theorem B.6. *Span equivalence (Algorithm B1) runs in time $O(k^2 \log k)$ if k is the total number of AST nodes in the basis translation.*

Proof. In the worst case, each of the $O(k)$ iterations of Algorithm B1 requires factoring, which is $O(k \log k)$ per Lemma B.5. \square

C Inlining Conditionals in Qwerty IR

For an example of the inlining technique described at the end of Section 5.4, consider lines 10 and 11 of Fig. C13. After lifting lambdas to functions, the IR produced by line 10 of Fig. C13 resembles the following:

```

1 @qpu
2 def teleport(secret: qubit) -> qubit:
3   alice, bob = 'p0' | '1' & std.flip
4
5   m_pm, m_std = \
6     secret + alice | '1' & std.flip \
7       | (pm + std).measure
8
9   secret_teleported = \
10    bob | (pm.flip if m_std else id) \
11    | (std.flip if m_pm else id)
12
13   return secret_teleported

```

Figure C13. Quantum teleportation in Qwerty. The syntax **std.flip** is syntactic sugar for **std** >> {'1', '0'}. The semantics of **pm.flip** is similar.

```

%23 = scf.if %22 {
  %28 = qwerty.func_const @lambda3[]
  scf.yield %28
} else {
  %28 = qwerty.func_const @lambda4[]
  scf.yield %28
}
%24 = qwerty.call_indirect %23(%10)

```

Clearly, this does not resemble the canonicalization pattern of a **call_indirect** with a **func_const** operand mentioned in Section 5.4 because there is an **scf.if** in the way. To address this, ASDF includes a specialized canonicalization pattern that transforms this IR into the following:

```

%24 = scf.if %22 {
  %28 = qwerty.func_const @lambda3[]
  %29 = qwerty.call_indirect %28(%10)
  scf.yield %29
} else {
  %28 = qwerty.func_const @lambda4[]
  %29 = qwerty.call_indirect %28(%10)
  scf.yield %29
}

```

Subsequently, the desired pattern is recognized and the indirect calls shown are converted to direct calls. Similar patterns are also implemented for the case when the result of an **scf.if** is passed to a **func_adj** or **func_pred**. Note that a similar transformation would be more difficult to implement in the presence of unstructured control flow (e.g., in QIR).

D Function Specialization Details

Section 6.2 describes how ASDF determines set of necessary function specializations, and Algorithm D5 shows this process as pseudocode. Because cyclic call graphs are not possible to construct in Qwerty, Algorithm D5 will always terminate.

Input: Qwerty IR after function specialization analysis
Output: Set of specializations
 (funcName, isAdj, numCtrls) to generate

```

1  $V, E \leftarrow \emptyset$ 
2 for every function  $f$  do
3    $V \leftarrow V \cup \{(\text{name of } f, \text{false}, 0)\}$ 
4 for every call and call_indirect  $op$  do
5   for every callee  $v'$  do
6      $V \leftarrow V \cup \{v'\}$ 
7      $E \leftarrow E \cup \{((\text{name of caller}, \text{false}, 0), v')\}$ 
8 repeat
9   for every function  $f$  do
10     $v \leftarrow (\text{name of } f, \text{false}, 0)$ 
11    for every edge  $(v, v') \in E$  do
12       $(\text{funcName}', \text{isAdj}', \text{numCtrls}') \leftarrow v'$ 
13      for every  $u \in V$  with name of  $f$  do
14         $(\text{funcName}, \text{isAdj}, \text{numCtrls}) \leftarrow u$ 
15         $v'' \leftarrow (\text{funcName}', \text{isAdj} \oplus \text{isAdj}',$ 
16           $\text{numCtrls} + \text{numCtrls}')$ 
17         $V \leftarrow V \cup \{v''\}$ 
18         $E \leftarrow E \cup \{(u, v'')\}$ 
19 until  $V$  and  $E$  stop changing
20 Run DFS from entry point and mark nodes reached
21 Delete unmarked nodes from  $V$ 
22 return  $V$ 

```

Algorithm D5: Determining function specializations needed to execute some Qwerty IR

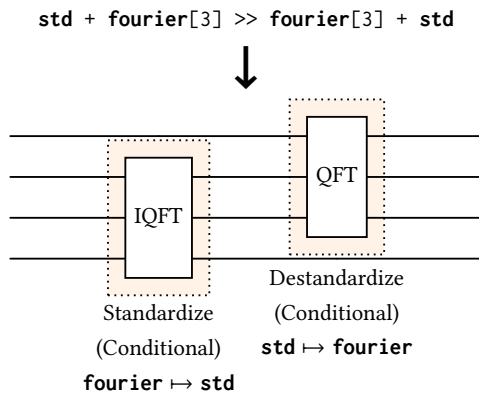


Figure E14. Compiling a basis translation with inseparable (de)standardizations

E Standardization Details

Section 6.3 gives some basic insight into the process of determining standardizations, but in realistic Qwerty compilation, the presence of *inseparable* primitive bases (a basis that cannot be written as a tensor product of smaller

Input: A well-typed basis translation $b_{\text{in}} \gg b_{\text{out}}$
Output: A list of standardizations and a list of destandardizations, where each element is a tuple (primBasis, dim, isConditional)

```

1 lstd, rstd  $\leftarrow []$ 
2 ldeque  $\leftarrow$  elements of  $b_{\text{in}}$ 
3 rdeque  $\leftarrow$  elements of  $b_{\text{out}}$ 
4 while ldeque and rdeque are not empty do
5    $\ell \leftarrow$  pop front of ldeque
6    $r \leftarrow$  pop front of rdeque
7   if neither  $\ell$  nor  $r$  are padding and
8     prim  $\ell =$  prim  $r$  then
9     kind  $\leftarrow$  Unconditional
10  else
11    kind  $\leftarrow$  Conditional
12  if dim  $\ell =$  dim  $r$  then
13    if  $\ell$  is not padding then
14      append (prim  $\ell$ , dim  $\ell$ , kind) to lstd
15    if  $r$  is not padding then
16      append (prim  $r$ , dim  $r$ , kind) to rstd
17  else
18    big  $\leftarrow \max(\ell, r)$ 
19    small  $\leftarrow \min(\ell, r)$ 
20     $\delta \leftarrow (\text{dim big}) - (\text{dim small})$ 
21    if prim big is separable and not padding then
22      if small is not padding then
23        append (prim small, dim small, kind)
24        to smallstd
25      append (prim big, dim small, kind) to
26      bigstd
27      push (prim big)[ $\delta$ ] to front of bigdeque
28    else
29      if small is not padding then
30        append (prim small, dim small,
31          Conditional) to smallstd
32      if big is not padding then
33        append (prim big, dim big,
34          Conditional) to bigstd
35      push padding[ $\delta$ ] to front of bigdeque
36  return lstd and rstd

```

Algorithm E6: Determining standardizations for a basis translation

bases) is a serious complication. For example, even though both three-qubit Fourier bases overlap in the basis translation $\text{std} + \text{fourier}[3] \gg \text{fourier}[3] + \text{std}$, there are no unconditional (de)standardizations. Instead, the compiler must synthesize a circuit (Fig. E14) invokes the inverse quantum Fourier transform (IQFT) on the rightmost three qubits

and then the quantum Fourier transform (QFT) on the leftmost three qubits. It would be invalid to try to run IQFT only on the rightmost qubit and then QFT only on the leftmost because the Fourier basis is inseparable.

Algorithm E6 handles the situation of standardizing in the presence of inseparable bases while also maintaining the invariant that the head of both dequeues start at the same qubit by delicately inserting padding basis elements when inseparable basis elements are encountered.

<pre> Input: A well-typed basis translation $b_{in} \gg b_{out}$ Output: An aligned basis translation $b'_{in} \gg b'_{out}$ 1 $b'_{in}, b'_{out} \leftarrow$ empty bases 2 ldeque \leftarrow elements of b_{in}, each standardized 3 rdeque \leftarrow elements of b_{out}, each standardized 4 while ldeque and rdeque are not empty do 5 $\ell \leftarrow$ pop front of ldeque 6 $r \leftarrow$ pop front of rdeque 7 if $\dim \ell = \dim r$ then 8 if $\ell = \mathbf{std}[N]$ and $r \neq \mathbf{std}[N]$ then 9 $\ell \leftarrow \mathbf{std}[N]$ as a basis literal 10 else if $\ell \neq \mathbf{std}[N]$ and $r = \mathbf{std}[N]$ then 11 $r \leftarrow \mathbf{std}[N]$ as a basis literal 12 $b'_{in} \leftarrow b'_{in} + \ell$ 13 $b'_{out} \leftarrow b'_{out} + r$ 14 else 15 $big \leftarrow \max(\ell, r)$ 16 $small \leftarrow \min(\ell, r)$ 17 if $big = \mathbf{std}[N]$ then 18 $factor \leftarrow \mathbf{std}[\dim small]$ 19 if $small \neq \mathbf{std}[N]$ then 20 $factor \leftarrow factor$ as a basis literal 21 $b'_{big} \leftarrow b'_{big} + factor$ 22 $b'_{small} \leftarrow b'_{small} + small$ 23 $\delta \leftarrow (\dim big) - (\dim small)$ 24 Push $\mathbf{std}[\delta]$ to front of bigdeque 25 else if a $(\dim small)$-dimensional basis literal $small'$ can be factored from big then 26 if $small = \mathbf{std}[N]$ then 27 $small \leftarrow small$ as a basis literal 28 $b'_{big} \leftarrow b'_{big} + small'$ 29 $b'_{small} \leftarrow b'_{small} + small$ 30 Push remainder to front of bigdeque 31 else 32 Merge until big' and $small'$ are basis elements of equal dimension 33 $b'_{big} \leftarrow b'_{big} + big'$ 34 $b'_{small} \leftarrow b'_{small} + small'$ 35 return $b'_{in} \gg b'_{out}$ </pre>	<p>Algorithm E7: Aligning basis translations</p>
---	---

F Basis Alignment Details

The permutation step of basis translation lowering as described in Section 6.3 can encounter some ambiguities. For example, consider the following basis translation:

$$\{'1'\} + \mathbf{std} \gg \{'11', '10'\}$$

The compiler must decide whether to interpret this as

$$\{'1'\} + \{'0', '1'\} \gg \{'1'\} + \{'1', '0'\}$$

or

$$\{'10', '11'\} \gg \{'11', '10'\}.$$

For the former, ASDF would synthesize a permutation that swaps $|0\rangle$ and $|1\rangle$ and then add a control afterward to honor the $\{'1'\}$ predicate. The latter would instead synthesize a permutation that swaps $|10\rangle$ and $|11\rangle$.

Alignment addresses this ambiguity by producing a functionally equivalent basis translation $b'_{in} \gg b'_{out}$ such that two conditions are met for each elementwise pair of basis elements be_{in} and be_{out} : first, $(\dim be_{in}) = (\dim be_{out})$; and second, be_{in} is a basis literal if and only if be_{out} is a basis literal. Both new basis translations in the previous paragraph are aligned forms of the first. However, factoring (the first aligned form above) is preferred over merging (the second aligned form) because a factored form is more structured; for instance, it can reduce the size of the permutation to synthesize. Factoring may not always be possible, however. For example, imagine the basis translation

$$\{'0', '1'\} + \{'0', '1'\} \gg \{'00', '10', '01', '11'\}.$$

The right-hand side cannot be written as the tensor product of two basis literals, so factoring is not possible. In such cases, the compiler resorts to merging (e.g., merging $\{'0', '1'\} + \{'0', '1'\}$ on the left-hand side of the previous example to form $\{'00', '01', '10', '11'\}$).

Algorithm E7 shows the procedure for aligning a basis translation. It attempts to factor if possible (lines 17 and 25), falling back to merging if necessary (line 32). *Standardizing* a basis element, mentioned on on lines 2 and 3, means changing its primitive basis to \mathbf{std} and removing all vector phases.

G Modifications Needed in QIR

When compiling to QIR, different function specializations are lowered to different LLVM functions. In accordance with the QIR callables API [20], a struct is generated for captures, and a table in static memory holds pointers to the different specializations of a given Qwerty function. The only modification to QIR needed by Qwerty is to modify the `__quantum__rt__callable_invoke` intrinsic not to manage arguments passed to the callable. In Q#, if f has type $\text{Qubit[]} \rightarrow \text{Unit}$, then `Controlled f` has type $(\text{Qubit}[], \text{Qubit}[]) \rightarrow \text{Unit}$, whereas in Qwerty, if f has type $\text{Qubit}[N] \rightarrow \text{Qubit}[N]$, then $b \ \& \ f$ has type $\text{Qubit}[M+N] \rightarrow \text{Qubit}[M+N]$ if $\dim b = M$ [2]. Thus, multiple uses of `&` for the same function in Qwerty only increase the size of the

qubit register argument, whereas in Q#, multiple uses of Controlled add more qubit arrays to the input tuple. In this case, QIR is hard-coded for Q# and attempts to collapse many qubit array arguments into one qubit array of controls, which is incorrect for QIR generated by ASDF.

References

- [1] Ali Javadi Abhari, Arvin Faruque, Mohammad Javad Dousti, Lukas Svec, Oana Catu, Amlan Chakrabati, Chen-Fu Chiang, Seth Vanderwilt, John Black, Fred Chong, Margaret Martonosi, Martin Suchara, Ken Brown, Massoud Pedram, and Todd Brun. 2012. *Scaffold: Quantum Programming Language*. Technical Report. Princeton University Department of Computer Science. 43 pages.
- [2] Austin J. Adams, Sharjeel Khan, Jeffrey S. Young, and Thomas M. Conte. 2024. Qwerty: A Basis-Oriented Quantum Programming Language. <http://arxiv.org/abs/2404.12603>
- [3] QIR Alliance. 2022. The QIR Alliance. <https://www.qir-alliance.org/alliance/>
- [4] Sheldon Axler. 2023. *Linear Algebra Done Right* (fourth edition ed.). Springer International Publishing.
- [5] Charles H. Bennett. 1989. Time/Space Trade-Offs for Reversible Computation. *SIAM J. Comput.* 18, 4 (Aug. 1989), 766–776. <https://doi.org/10.1137/0218053>
- [6] Ethan Bernstein and Umesh Vazirani. 1993. Quantum complexity theory. In *Proceedings of the twenty-fifth annual ACM symposium on Theory of Computing (STOC '93)*. Association for Computing Machinery, New York, NY, USA, 11–20. <https://doi.org/10.1145/1677088.1677097>
- [7] Xiaoning Bian. 2020. quipper-qasm: Flatten Quipper ASCII format circuit into a list of gates. <https://github.com/onestruggler/quipper-qasm/>
- [8] Sonia Lopez Bravo. 2024. QIR Target Profile Types - Azure Quantum. Microsoft. <https://learn.microsoft.com/en-us/azure/quantum/quantum-computing-target-profiles>
- [9] Andrew Cross, Ali Javadi-Abhari, Thomas Alexander, Niel De Beaudrap, Lev S. Bishop, Steven Heidel, Colm A. Ryan, Prasahnt Sivarajah, John Smolin, Jay M. Gambetta, and Blake R. Johnson. 2022. OpenQASM 3: A Broader and Deeper Quantum Assembly Language. *ACM Transactions on Quantum Computing* 3, 3 (Sept. 2022), 12:1–12:50. <https://doi.org/10.1145/3505636>
- [10] Andrew W. Cross, Lev S. Bishop, John A. Smolin, and Jay M. Gambetta. 2017. *Open Quantum Assembly Language*. Technical Report. arXiv. <http://arxiv.org/abs/1707.03429>
- [11] David Deutsch and Richard Jozsa. 1997. Rapid solution of problems by quantum computation. *Proceedings of the Royal Society of London. Series A: Mathematical and Physical Sciences* 439, 1907 (Jan. 1997), 553–558. <https://doi.org/10.1098/rspa.1992.0167>
- [12] S. D. Fallek, C. D. Herold, B. J. McMahon, K. M. Maller, K. R. Brown, and J. M. Amini. 2016. Transport implementation of the Bernstein–Vazirani algorithm with ion qubits. *New Journal of Physics* 18, 8 (Aug. 2016), 083030. <https://doi.org/10.1088/1367-2630/18/8/083030>
- [13] Python Software Foundation. 2023. ast – Abstract Syntax Trees. <https://docs.python.org/3/library/ast.html>
- [14] Austin G. Fowler, Matteo Mariantoni, John M. Martinis, and Andrew N. Cleland. 2012. Surface codes: Towards practical large-scale quantum computation. *Physical Review A* 86, 3 (Sept. 2012), 032324. <https://doi.org/10.1103/PhysRevA.86.032324>
- [15] Alexander S. Green, Peter LeFanu Lumsdaine, Neil J. Ross, Peter Selinger, and Benoît Valiron. 2013. An Introduction to Quantum Programming in Quipper. In *Reversible Computation*, Gerhard W. Dueck and D. Michael Miller (Eds.). Springer, Berlin, Heidelberg, 110–124. https://doi.org/10.1007/978-3-642-38986-3_10
- [16] Alexander S. Green, Peter LeFanu Lumsdaine, Neil J. Ross, Peter Selinger, and Benoît Valiron. 2013. Quipper: a scalable quantum programming language. In *Proceedings of the 34th ACM SIGPLAN Conference on Programming Language Design and Implementation (PLDI '13)*. Association for Computing Machinery, New York, NY, USA, 333–342. <https://doi.org/10.1145/2491956.2462177>
- [17] Lov K. Grover. 1996. A fast quantum mechanical algorithm for database search. In *Proceedings of the twenty-eighth annual ACM symposium on Theory of Computing (STOC '96)*. Association for Computing Machinery, New York, NY, USA, 212–219. <https://doi.org/10.1145/237814.237866>
- [18] Lov K. Grover. 1997. Quantum Mechanics Helps in Searching for a Needle in a Haystack. *Physical Review Letters* 79, 2 (July 1997), 325–328. <https://doi.org/10.1103/PhysRevLett.79.325>
- [19] Michael B. Healy, Reza Jokar, Soolu Thomas, Vincent R. Pascuzzi, Kit Barton, Thomas A. Alexander, Roy Elkabetz, Brian C. Donovan, Hiroshi Horii, and Marius Hillenbrand. 2024. Design and architecture of the IBM Quantum Engine Compiler. <https://doi.org/10.48550/arXiv.2408.06469>
- [20] Bettina Heim. 2022. QIR: Callables. https://github.com/qir-alliance/qir-spec/blob/8b75546ad25a5bb243edf6fab80bd356856a7b24/specification/v0.1/2_Callables.md
- [21] Bettina Heim. 2022. QIR Specification. <https://github.com/qir-alliance/qir-spec>.
- [22] David Ittah, Ali Asadi, Erick Ochoa Lopez, Sergei Mironov, Samuel Banning, Romain Moyard, Mai Jacob Peng, and Josh Izaac. 2024. Catalyst: a Python JIT compiler for auto-differentiable hybrid quantum programs. *Journal of Open Source Software* 9, 99 (July 2024), 6720. <https://doi.org/10.21105/joss.06720>
- [23] David Ittah, Thomas Häner, Vadym Kliuchnikov, and Torsten Hoefler. 2022. QIRO: A Static Single Assignment-based Quantum Program Representation for Optimization. *ACM Transactions on Quantum Computing* 3, 3 (July 2022), 14:1–14:32. <https://doi.org/10.1145/3491247>
- [24] Ali JavadiAbhari, Shruti Patil, Daniel Kudrow, Jeff Heckey, Alexey Lvov, Frederic T. Chong, and Margaret Martonosi. 2014. Scaffold: a framework for compilation and analysis of quantum computing programs. In *Proceedings of the 11th ACM Conference on Computing Frontiers (CF '14)*. Association for Computing Machinery, New York, NY, USA, 1–10. <https://doi.org/10.1145/2597917.2597939>
- [25] Chris Lattner and Vikram Adve. 2004. LLVM: A Compilation Framework for Lifelong Program Analysis & Transformation. In *Proceedings of the international symposium on Code generation and optimization: feedback-directed and runtime optimization (CGO '04)*. IEEE Computer Society, USA, 75.
- [26] Chris Lattner, Mehdi Amini, Uday Bondhugula, Albert Cohen, Andy Davis, Jacques Pienaar, River Riddle, Tatiana Shpeisman, Nicolas Vasilache, and Oleksandr Zinenko. 2021. MLIR: Scaling Compiler Infrastructure for Domain Specific Computation. In *2021 IEEE/ACM International Symposium on Code Generation and Optimization (CGO)*. Association for Computing Machinery, New York, NY, USA, 2–14. <https://doi.org/10.1109/CGO51591.2021.9370308>
- [27] Ji Liu, Luciano Bello, and Huiyang Zhou. 2021. Relaxed Peephole Optimization: A Novel Compiler Optimization for Quantum Circuits. In *2021 IEEE/ACM International Symposium on Code Generation and Optimization (CGO)*. 301–314. <https://doi.org/10.1109/CGO51591.2021.9370310>
- [28] Thomas Lubinski, Cassandra Granade, Amos Anderson, Alan Geller, Martin Roetteler, Andrei Petrenko, and Bettina Heim. 2022. Advancing hybrid quantum–classical computation with real-time execution. *Frontiers in Physics* 10 (2022), 940293. <https://www.frontiersin.org/articles/10.3389/fphy.2022.940293>
- [29] Alexander McCaskey and Thien Nguyen. 2021. A MLIR Dialect for Quantum Assembly Languages. In *2021 IEEE International Conference on Quantum Computing and Engineering (QCE)*. IEEE, Seoul, Korea,

- 255–264. <https://doi.org/10.1109/QCE52317.2021.00043>
- [30] Alexander J. McCaskey, Dmitry I. Lyakh, Eugene F. Dumitrescu, Sarah S. Powers, and Travis S. Humble. 2020. XACC: a system-level software infrastructure for heterogeneous quantum–classical computing. *Quantum Science and Technology* 5, 2 (Feb. 2020), 024002. <https://doi.org/10.1088/2058-9565/ab6bf6>
- [31] Giulia Meuli, Mathias Soeken, Earl Campbell, Martin Roetteler, and Giovanni de Micheli. 2019. The Role of Multiplicative Complexity in Compiling Low T-count Oracle Circuits. In *2019 IEEE/ACM International Conference on Computer-Aided Design (ICCAD)*. 1–8. <https://doi.org/10.1109/ICCAD45719.2019.8942093>
- [32] Microsoft. 2024. *Azure Quantum Development Kit*. <https://github.com/microsoft/qsharp>
- [33] D. Michael Miller, Dmitri Maslov, and Gerhard W. Dueck. 2003. A transformation based algorithm for reversible logic synthesis. In *Proceedings of the 40th annual Design Automation Conference (DAC '03)*. Association for Computing Machinery, New York, NY, USA, 318–323. <https://doi.org/10.1145/775832.775915>
- [34] Michael A. Nielsen and Isaac L. Chuang. 2010. *Quantum Computation and Quantum Information: 10th Anniversary Edition* (1st edition ed.). Cambridge University Press, Cambridge ; New York.
- [35] Jennifer Paykin, Robert Rand, and Steve Zdancewic. 2017. QWIRE: a core language for quantum circuits. *ACM SIGPLAN Notices* 52, 1 (Jan. 2017), 846–858. <https://doi.org/10.1145/3093333.3009894>
- [36] Anurudh Peduri, Siddharth Bhat, and Tobias Grosser. 2022. QSSA: an SSA-based IR for Quantum computing. In *Proceedings of the 31st ACM SIGPLAN International Conference on Compiler Construction (CC 2022)*. Association for Computing Machinery, New York, NY, USA, 2–14. <https://doi.org/10.1145/3497776.3517772>
- [37] Will Powell, Jason Riedy, Jeffrey S. Young, and Thomas M. Conte. 2019. Wrangling Rogues: A Case Study on Managing Experimental Post-Moore Architectures. In *Practice and Experience in Advanced Research Computing 2019: Rise of the Machines (learning) (PEARC '19)*. Association for Computing Machinery, New York, NY, USA, 1–8. <https://doi.org/10.1145/3332186.3332223>
- [38] Qiskit contributors. 2023. Qiskit: An Open-source Framework for Quantum Computing. <https://doi.org/10.5281/zenodo.2573505>
- [39] River Riddle and Matthias Springer. 2021. Writing DataFlow Analyses in MLIR. <https://mlir.llvm.org/docs/Tutorials/DataFlowAnalysis/>
- [40] Bruno Schmitt and Giovanni De Micheli. 2022. tweedledum: A Compiler Companion for Quantum Computing. In *2022 Design, Automation & Test in Europe Conference & Exhibition (DATE)*. IEEE, Antwerp, Belgium, 7–12. <https://doi.org/10.23919/DATE54114.2022.9774510>
- [41] Bruno Schmitt, Ali Javadi-Abhari, and Giovanni De Micheli. 2021. Compilation flow for classically defined quantum operations. In *2021 Design, Automation & Test in Europe Conference & Exhibition (DATE)*. 964–967. <https://doi.org/10.23919/DATE51398.2021.9474163>
- [42] Peter Selinger. 2013. Quantum circuits of T-depth one. *Physical Review A* 87, 4 (April 2013), 042302. <https://doi.org/10.1103/PhysRevA.87.042302>
- [43] Peter Selinger and Benoit Valiron. 2006. A lambda calculus for quantum computation with classical control. *Mathematical Structures in Computer Science* 16, 3 (June 2006), 527–552. <https://doi.org/10.1017/S0960129506005238>
- [44] V.V. Shende, S.S. Bullock, and I.L. Markov. 2006. Synthesis of quantum-logic circuits. *IEEE Transactions on Computer-Aided Design of Integrated Circuits and Systems* 25, 6 (June 2006), 1000–1010. <https://doi.org/10.1109/TCAD.2005.855930>
- [45] Safat Siddiqui, Mohammed Jahiril Islam, and Omar Shehab. 2014. Five Quantum Algorithms Using Quipper. <https://doi.org/10.48550/arXiv.1406.4481>
- [46] D.R. Simon. 1994. On the power of quantum computation. In *Proceedings 35th Annual Symposium on Foundations of Computer Science*. 116–123. <https://doi.org/10.1109/SFCS.1994.365701>
- [47] Daniel R. Simon. 1997. On the Power of Quantum Computation. *SIAM J. Comput.* 26, 5 (Oct. 1997), 1474–1483. <https://doi.org/10.1137/S0097539796298637>
- [48] Kartik Singhal, Kesha Hietala, Sarah Marshall, and Robert Rand. 2022. Q# as a Quantum Algorithmic Language. <http://arxiv.org/abs/2206.03532>
- [49] Robert S. Smith, Michael J. Curtis, and William J. Zeng. 2017. *A Practical Quantum Instruction Set Architecture*. Technical Report arXiv:1608.03355. arXiv. <http://arxiv.org/abs/1608.03355>
- [50] Mathias Soeken, Gerhard W. Dueck, and D. Michael Miller. 2016. A Fast Symbolic Transformation Based Algorithm for Reversible Logic Synthesis. In *Reversible Computation*, Simon Devitt and Ivan Lanese (Eds.). Springer International Publishing, Cham, 307–321. https://doi.org/10.1007/978-3-319-40578-0_22
- [51] Mathias Soeken and Mariia Mykhailova. 2022. Automatic oracle generation in microsoft’s quantum development kit using QIR and LLVM passes. In *Proceedings of the 59th ACM/IEEE Design Automation Conference (San Francisco, California) (DAC '22)*. Association for Computing Machinery, New York, NY, USA, 1363–1366. <https://doi.org/10.1145/3489517.3530626>
- [52] Mathias Soeken, Heinz Riene, Winston Haaswijk, Eleonora Testa, Bruno Schmitt, Giulia Meuli, Fereshte Mozafari, Siang-Yun Lee, Alessandro Tempia Calvino, Dewmini Sudara Marakkalage, and Giovanni De Micheli. 2022. The EPFL Logic Synthesis Libraries. <http://arxiv.org/abs/1805.05121>
- [53] Krysta Svore, Alan Geller, Matthias Troyer, John Azariah, Christopher Granade, Bettina Heim, Vadym Kliuchnikov, Mariia Mykhailova, Andres Paz, and Martin Roetteler. 2018. Q#: Enabling Scalable Quantum Computing and Development with a High-level DSL. In *Proceedings of the Real World Domain Specific Languages Workshop 2018 (RWDSL2018)*. Association for Computing Machinery, New York, NY, USA, 1–10. <https://doi.org/10.1145/3183895.3183901>
- [54] Eduardo González Sánchez and Bradben. 2024. Q# Specialization declarations. <https://learn.microsoft.com/en-us/azure/quantum/user-guide/language/programstructure/specializationdeclarations>
- [55] The CUDA-Q development team. 2024. *CUDA-Q*. <https://github.com/NVIDIA/cuda-quantum>
- [56] Philippe Tillet, H. T. Kung, and David Cox. 2019. Triton: an intermediate language and compiler for tiled neural network computations. In *Proceedings of the 3rd ACM SIGPLAN International Workshop on Machine Learning and Programming Languages (MAPL 2019)*. Association for Computing Machinery, New York, NY, USA, 10–19. <https://doi.org/10.1145/3315508.3329973>
- [57] Wim van Dam, Mariia Mykhailova, and Mathias Soeken. 2023. Using Azure Quantum Resource Estimator for Assessing Performance of Fault Tolerant Quantum Computation. In *Proceedings of the SC '23 Workshops of The International Conference on High Performance Computing, Network, Storage, and Analysis (SC-W '23)*. Association for Computing Machinery, New York, NY, USA, 1414–1419. <https://doi.org/10.1145/3624062.3624211>
- [58] Stefan Wernli and Ian Davis. 2024. QIR Runner. <https://github.com/qir-alliance/qir-runner>.
- [59] Stefan Wernli and Bettina Heim. 2022. QIR Specification. https://github.com/qir-alliance/qir-spec/blob/11db5f743d637f/specification/under_development/profiles/Base_Profile.md
- [60] Filip Wojcieszyn. 2022. *Introduction to Quantum Computing with Q# and QDK*. Springer International Publishing, Cham. <https://doi.org/10.1007/978-3-030-99379-5>
- [61] Elaine Wong, Vicente Leyton Ortega, Daniel Claudino, Seth Johnson, Sharmin Afrose, Meenambika Gowrishankar, Anthony M. Cabrera, and Travis S. Humble. 2024. A Cross-Platform Execution Engine for the Quantum Intermediate Representation. <https://doi.org/10.48550/arXiv.2404.14299>

- [62] James R. Wootton, Francis Harkins, Nicholas T. Bronn, Almudena Carrera Vazquez, Anna Phan, and Abraham T. Asfaw. 2021. Teaching quantum computing with an interactive textbook. In *2021 IEEE International Conference on Quantum Computing and Engineering (QCE)*. 385–391. <https://doi.org/10.1109/QCE52317.2021.00058>
- [63] Jeffrey S. Young, Jason Riedy, Thomas M. Conte, Vivek Sarkar, Prasanth Chatarasi, and Sriseshan Srikanth. 2019. Experimental Insights from the Rogues Gallery. In *2019 IEEE International Conference on Rebooting Computing (ICRC)*. 1–8. <https://doi.org/10.1109/ICRC.2019.8914707>
- [64] Charles Yuan, Christopher McNally, and Michael Carbin. 2022. Twist: sound reasoning for purity and entanglement in Quantum programs. *Proceedings of the ACM on Programming Languages* 6, POPL (Jan. 2022), 30:1–30:32. <https://doi.org/10.1145/3498691>
- [65] Tong Zhou, Jun Shirako, Anirudh Jain, Sriseshan Srikanth, Thomas M. Conte, Richard Vuduc, and Vivek Sarkar. 2020. Intrepydd: performance, productivity, and portability for data science application kernels. In *Proceedings of the 2020 ACM SIGPLAN International Symposium on New Ideas, New Paradigms, and Reflections on Programming and Software*. ACM, Virtual USA, 65–83. <https://doi.org/10.1145/3426428.3426915>